END

FILM

DTIC

MICROCOPY RESOLUTION TEST CHART

NATIONAL BUREAU OF STANDARDS 1963-A

Dynamics of Space Charge Waves in the Laser Beat Wave Accelerator

C. M. TANG AND P. SPRANGLE

Plasma Theory Branch
Plasma Physics Division

R. N. SUDAN

Laboratory for Plasma Studies
Cornell University
Ithaca, NY 14853

AD-A149 688

January 30, 1985

DTIC FILE COPY

NAVAL RESEARCH LABORATORY
Washington, D.C.

DTIC
ELECTE
JAN 3 1 1985
A

85   01   23   057

REPORT DOCUMENTATION PAGE

1a. REPORT SECURITY CLASSIFICATION UNCLASSIFIED		1b. RESTRICTIVE MARKINGS			
2a. SECURITY CLASSIFICATION AUTHORITY		3. DISTRIBUTION / AVAILABILITY OF REPORT Approved for public release; distribution unlimited.			
2b. DECLASSIFICATION / DOWNGRADING SCHEDULE					
4. PERFORMING ORGANIZATION REPORT NUMBER(S) NRL Memorandum Report 5324		5. MONITORING ORGANIZATION REPORT NUMBER(S)			
6a. NAME OF PERFORMING ORGANIZATION Naval Research Laboratory	6b. OFFICE SYMBOL (If applicable) Code 4790	7a. NAME OF MONITORING ORGANIZATION Department of Energy			
6c. ADDRESS (City, State, and ZIP Code) Washington, DC 20375-5000		7b. ADDRESS (City, State, and ZIP Code) Washington, DC 20545			
8a. NAME OF FUNDING / SPONSORING ORGANIZATION Department of Energy	8b. OFFICE SYMBOL (If applicable)	9. PROCUREMENT INSTRUMENT IDENTIFICATION NUMBER			
8c. ADDRESS (City, State, and ZIP Code) Washington, DC 20545		10. SOURCE OF FUNDING NUMBERS			
		PROGRAM ELEMENT NO	PROJECT NO DE-AI05 83ER40117	TASK NO	WORK UNIT ACCESSION NO DN380-537

11. TITLE (Include Security Classification)

Dynamics of Space Charge Waves in the Laser Beat Wave Accelerator

12. PERSONAL AUTHOR(S)
Tang, C.M., Sprangle, P. and Sudan, R.N.*

13a. TYPE OF REPORT Interim	13b. TIME COVERED FROM _____ TO _____	14. DATE OF REPORT (Year, Month, Day) 1985 January 30	15. PAGE COUNT 51

16. SUPPLEMENTARY NOTATION *Laboratory for Plasma Studies, Cornell University, Ithaca, NY 14853

This work was sponsored by the U. S. Department of Energy.

17.	COSATI CODES		18. SUBJECT TERMS (Continue on reverse if necessary and identify by block number)
FIELD	GROUP	SUB-GROUP	Laser beat wave accelerator
			Large amplitude plasma waves

19. ABSTRACT (Continue on reverse if necessary and identify by block number)

The excitation of plasma waves by two laser beams, whose frequency difference is approximately the plasma frequency, is analyzed. Our nonlinear analysis is fully relativistic in the axial and transverse directions and includes mismatching of the laser beat frequency to the plasma frequency, time dependent laser amplitudes, and an applied transverse magnetic field (surfatron configuration). Our analytical results for the large amplitude plasma waves includes an axial constant of motion, accelerating electric field, and its phase velocity. The analytical results in the weak laser power limit are in good agreement with numerical results obtained from the complete equations. The imposed transverse magnetic field is found to increase the effective plasma frequency, but has little effect on the plasma dynamics.

20. DISTRIBUTION / AVAILABILITY OF ABSTRACT ☒ UNCLASSIFIED/UNLIMITED ☐ SAME AS RPT ☐ DTIC USERS	21. ABSTRACT SECURITY CLASSIFICATION UNCLASSIFIED	
22a. NAME OF RESPONSIBLE INDIVIDUAL Cha-Mei Tang	22b. TELEPHONE (Include Area Code) (202) 767-4148	22c. OFFICE SYMBOL Code 4790

DD FORM 1473, 84 MAR
83 APR edition may be used until exhausted
All other editions are obsolete

CONTENTS

DYNAMICS OF SPACE CHARGE WAVES IN THE
LASER BEAT WAVE ACCELERATOR

I. Introduction

The laser beat wave accelerator is one of a number of laser driven particle accelerating schemes,[1,2] which is currently receiving considerable attention. Existing types of synchrotron and linear accelerators are nearing their economic limits in going much beyond a few TeV in energies. The availability of high power laser beams ($\geq 10^{14}$ watts) with electric fields as high as 10^9V/cm brings about the possibility of using these high fields to accelerate particles. Direct use of these fields for continuous particle acceleration is not possible due to the transverse polarization and rapid oscillation of the fields. A number of laser driven acceleration schemes have been suggested over the past two dozen years.

. Before describing the laser beat wave accelerator concept a brief description of some of the other generic laser acceleration concepts are mentioned. These include the inverse free electron laser accelerator, the grating accelerator, the inverse Cerenkov accelerator, the cyclotron resonance accelerator and the use of high gradient short wavelength structures.

In the inverse free electron laser accelerator scheme,[3-5] an electron beam together with an intense laser pulse is propagated through a spatially periodic magnetic field known as a wiggler field. The wiggler period and laser wavelength are such that the transverse particle velocity due to the wiggler field is in phase with the transverse electric field of the laser radiation. By appropriately contouring both the wiggler amplitude and period, the injected particles can be continually accelerated. The inverse of this process has been used to generate radiation and is the well-known free electron laser mechanism.

The grating accelerator mechanism[6] relies on the fact that when electro-magnetic radiation propagates along a diffraction grating a slow electro-

1

magnetic surface wave is excited along the grating's surface. This scheme
utilizes the slow, phase velocity less than the speed of light, electro-
magnetic wave to trap and accelerate a beam of injected electrons.

The inverse Cerenkov accelerator[7,8] approach takes advantage of the fact
that the index of refraction of a neutral gas is slightly greater than
unity. The laser radiation within the gas has a phase velocity less than the
speed of light making it possible to trap and accelerate an injected beam of
particles.

In the cyclotron resonance accelerator mechanism[9,10] an electron beam is
injected along a uniform magnetic field together with a parallel propagating
laser beam. Because of a self resonance effect, the phase of the electron's
transverse velocity can be synchronized with the radiation electric field.
This synchronism is maintained throughout the acceleration length.

The high gradient short wavelength structure concept[11] is basically a
scaled down version of a conventional slow wave accelerator structure.
Radiation power sources in the centimeter wavelength range appear appropriate
for this approach. The potential advantage of this scheme is that due to the
short wavelength employed, relatively low radiation energy per unit length is
needed to fill the small structure, and breakdown field limits appear to be
higher.

The laser beat wave accelerator concept is a collective acceleration
scheme which utilizes a large amplitude plasma wave with phase velocity
slightly less than the velocity of light to accelerate charged particles. The
large amplitude plasma wave is generated by the nonlinear coupling of two
intense laser beams propagating through the plasma.[1-2,12-22] In this process
the two laser beams with frequencies ω_1, ω_2 and corresponding wavenumbers k_1,
k_2 couple through the plasma to produce a ponderomotive wave with frequency

$\omega_1 - \omega_2$ and wavenumber $k_1 - k_2$. See Fig. 1. If $\omega_1 - \omega_2 \simeq \omega_p$, the plasma wave will initially grow linearly in time. If the laser frequencies are much greater than the ambient plasma frequency ω_p then the phase velocity of the ponderomotive wave is nearly equal to the group velocity of the laser wave. In this scheme a beam of injected electrons with axial velocity close to the plasma wave phase velocity can be accelerated until synchronism is lost.

A potentially attractive variation of the plasma beat wave accelerator is the surfatron scheme.[22] In the surfatron configuration a transverse magnetic field is externally applied permitting the accelerated particles to effectively $\underset{\sim}{E} \times \underset{\sim}{B}$ drift in a direction transverse to the laser propagation direction. In this configuration the electrons can remain in phase with the plasma wave allowing, in principle, higher electron energies to be achieved.

In this paper, we analyze the build-up of the plasma waves, extending the analysis of Rosenbluth and Liu.[23,24] Our nonlinear, fully relativistic treatment of the plasma wave includes mismatching of the laser beat frequencies to the plasma frequency, applied transverse magnetic field as well as time-dependent laser pulses. The resultant equations in Section II describe the growth of the excited plasma waves up until saturation. We find that the effective plasma frequency is increased from the ambient plasma frequency when a transverse magnetic field is applied. On the other hand, the effective plasma frequency can be decreased as the transverse motion, induced by intense laser powers, becomes relativistic.

Making the weak laser power approximation in Section III, we obtain analytical results for the initial growth rate for the large-amplitude plasma wave, the maximum accelerating electric field, the laser beat frequency requirement and the corresponding phase velocity. As the combined laser powers (measured by ε) increases, the maximum amplitude of the plasma electric

3

field increases as $\alpha\varepsilon^{1/3}$. The variable α is a function of frequency mismatch between the laser beat frequency and the effective plasma frequency. The relativistic effect associated with the transverse motion is incorporated in the parameter ε. In the limit of exact resonance and nonrelativistic motion in the transverse direction, we confirm the results of Rosenbluth and Liu.[24] For the purpose of accelerating electrons, it is desirable not only to have the largest accelerating electric field but also the phase velocity, v_{ph}, less than but close to the speed of light. We find, however, that as the amplitude of the plasma wave gets larger, the corresponding phase velocities become slower i.e., $v_g - v_{ph}$ scales as $\varepsilon^{2/3}$, where v_g is the group velocity of the lasers in the plasma. The maximum accelerating field for a given laser power parameter ε is achieved when the laser beat frequency is less than the effective plasma frequency. The difference between the effective plasma frequency and the optimal laser beat frequency is proportional to $\varepsilon^{2/3}$. The plasma build-up time is proportional to $\varepsilon^{-2/3}$. The analytical results also shows that the transverse magnetic field has little effect on the plasma dynamics to the lowest order.

In Section IV, we obtained numerical results from the full treatment and compared them with the analytical results. In the weak laser power limit, the results are in excellent agreement. We observe the wave steepening phenomenon caused by relativistic effects. As the laser power increases, the waves eventually break and become turbulent. We show that for laser pulse lengths much longer than the plasma wave build-up time, the amplitude and the phase velocity of the plasma waves are oscillatory. By applying lasers with pulse lengths approximately equal to the plasma wave build-up time, both the amplitude and phase velocity can be approximately maintained at a constant value.

II. Plasma Beat Wave Accelerator

Our model consists of a spatially one-dimensional plasma containing infinitely massive ions. Initially the plasma is assumed to be cold, uniform in density and stationary. Large amplitude plasma waves are excited by the ponderomotive force associated with the two laser pulses. Using a Lagrangian formulation, the temporal evolution of the plasma wave over a single spatial period is studied at a fixed axial position.

This analysis treats the following topics: 1) nonlinear behavior of plasma waves, 2) relativistic effects, 3) effect of finite duration laser pulses, 4) mismatching of the laser beat frequency to the plasma frequency, and 5) the effect of an applied transverse magnetic field.

A. Non-Linear, Relativistic Plasma Dynamics

The vector potential associated with the linearly polarized laser pulses within the plasma is

$$\underset{\sim}{A}_L(z,t) = \sum_{i=1,2} A_i(z - v_g t) \cos(k_i z - \omega_i t + \phi_i) \hat{e}_x, \tag{1}$$

where $A_i(z - v_g t)$ denotes the pulse amplitude of the i_{th} laser, $\omega_i \gg \omega_p$, ω_i is the laser frequency, $\omega_p = (4\pi |e|^2 n_o/m_o)^{1/2}$ is the ambient plasma frequency, n_o is the ambient electron density, and $v_g = (\omega_1 - \omega_2)/(k_1 - k_2)$ is the group velocity of the laser radiation. In our model, we assume k_i to be constant and A_i specified, i.e., the imposed laser fields are assumed to be unaffected by the plasma density modulations. This is a good approximation if $\omega_i \gg \omega_p$, $|e|A_i/(m_o c^2) < 1$ and $\delta n/n_o < 1$, where δn is the plasma density modulation. Also included in our model is an applied transverse static magnetic field which is represented by the vector potential

5

$$A_o = B_o z \, \hat{e}_y. \tag{2}$$

The electric and magnetic fields in terms of the vector potential are $E = - \frac{1}{c} \frac{\partial}{\partial t} A_L$ and $B = \nabla \times (A_L + A_o)$ respectively. In our configuration, the electric field vector is parallel to the transverse magnetic field, $E_L \parallel B_o$.

In our one-dimensional model, the transverse particle dynamics possess two constants of motion, i.e., the canonical momentum in the x and y direction,

$$C_\perp = - \frac{|e|}{c} (A_L + A_o) + P_\perp . \tag{3}$$

Assuming that $P_\perp = 0$ prior to the arrival of the laser pulses, it follows that the electron's transverse momenta are given by

$$P_x = \frac{|e|}{c} A_L \cdot \hat{e}_x , \tag{4}$$

and

$$P_y = \frac{|e|}{c} B_o (z-z_o), \tag{5}$$

where z_o is the initial axial position of the electron.

The momentum equation in the axial direction can now be written as

$$\frac{dp_z}{dt} = -|e| \, E_z - \frac{|e|}{\gamma m_o c} (P_x \frac{\partial A_x}{\partial z} + P_y \frac{\partial A_y}{\partial z}), \tag{6}$$

where E_z is the self-consistent plasma induced electric field, $A_x = A_L \cdot \hat{e}_x$ and $A_y = B_o z$. The particle energy equation is

6

$$\frac{d\gamma}{dt} = \frac{|e|}{\gamma m_o^2 c^3} \ (P_x \frac{\partial A_x}{\partial t} + P_y \frac{\partial A_y}{\partial t}) - \frac{|e|}{\gamma m_o^2 c^2} P_z E_z. \tag{7}$$

Combining (6) and (7), we obtain the equation governing the axial motion of the electrons,

$$\frac{d\beta_z}{dt} = - \frac{|e|}{m_o c} \ \frac{(1 - \beta_z^2)^{3/2}}{(1 + U_x^2 + U_y^2)^{1/2}} \ E_z - \frac{c \ (1 - \beta_z^2)}{2(1 + U_x^2 + U_y^2)} \ (\frac{\partial}{\partial z} + \frac{\beta_z}{c} \frac{\partial}{\partial t}) \ (U_x^2 + U_y^2),$$

$$\tag{8}$$

where $\beta_z = v_z/c$, $U_x = \frac{|e|}{m_o c^2} \ \underset{\sim}{A}_L \cdot \hat{e}_x$, and $U_y = - \frac{|e|}{m_o c^2} \ B_o(z-z_o)$.

Neglecting nonresonant terms we find that

$$U_x^2 + U_y^2 = \frac{\Omega^2}{c^2} \ (z-z_o)^2 + \frac{1}{2} \ (a_1^2 + a_2^2) + a_1 a_2 \cos (\Delta kz - \Delta \omega t + \Delta \phi), \tag{9}$$

where $\Omega = |e| B_o/m_o c$ is the cyclotron frequency, $a_i = |e| A_i(z - v_g t)/m_o c^2$, $\Delta k = k_1 - k_2$, $\Delta \omega = \omega_1 - \omega_2$, $\Delta \phi = \phi_1 - \phi_2$, and $\beta_g = \Delta \omega/c \Delta k$. The difference in the laser frequencies is assumed to be close to the plasma frequency, $\Delta \omega \approx \omega_p$. Substituting (9) into (8), yields

$$\frac{d\beta_z}{dt} = - \frac{|e|}{m_o c} \frac{(1-\beta_z^2)^{3/2}}{\gamma_\perp} E_z - \frac{(1-\beta_z^2)}{\gamma_\perp^2} \ \frac{\Omega^2}{c} \ (z-z_o)$$

$$\tag{10}$$

$$+ c \ \frac{(1-\beta_z^2)}{2\gamma_\perp^2} (\frac{\partial}{\partial z} + \frac{\beta_z}{c} \frac{\partial}{\partial t}) \left[\frac{1}{2}(a_1^2 + a_2^2) + a_1 a_2 \cos(\Delta kz - \Delta \omega t + \Delta \phi) \right],$$

where

$$\gamma_\perp = (1 + U_x^2 + U_y^2)^{1/2} \tag{11}$$

7

$$= \left[1 + \frac{\Omega^2}{c^2} (z-z_0)^2 + \frac{1}{2} (a_1^2 + a_2^2) + a_1 a_2 \cos(\Delta kz - \Delta\omega t + \Delta\phi) \right]^{1/2}$$

is a measure of the magnitude of the transverse oscillations induced by the laser beams.

B. Transformation to Lagrangian Variables

Equation (10) is expressed in terms of Eulerian independent variables z and t. It proves convenient at this point to perform a transformation to Lagrangian variables,[23,24] because the plasma induced field E_z takes on a particularly simple form. In the Lagrangian variables, the independent variables are z_0 and τ, such that

$$t = \tau, \tag{12}$$

$$z = z_0 + \xi(z_0, \tau),$$

where z_0 is the initial position of the electrons at $\tau = 0$ and $\xi(z_0, \tau)$ is the axial displacement at time τ relative to its initial position z_0. The axial electric field written in terms of the new variables (z_0, τ) is

$$E_z(z_0, \tau) = 4\pi |e| n_0 \, \xi(z_0, \tau). \tag{13}$$

The equation governing the plasma oscillations can now be written completely in terms of $\xi(z_0, \tau)$, i.e.,

$$\ddot{\xi} + \left[\omega_p^2 (1 - \frac{\dot{\xi}^2}{c^2})^{1/2} + \frac{\Omega^2}{\gamma_\perp} \right] \frac{(1 - \dot{\xi}^2/c^2)}{\gamma_\perp} \, \xi \tag{14}$$

$$= - \frac{(1 - \dot{\xi}^2/c^2)}{2\gamma_\perp^2} \left[c^2 (1 - \beta_g \, \dot{\xi}/c) \right] (a_1 + a_2 \cos \Delta\psi) \frac{\partial a_1(\alpha)}{\partial \alpha}$$

8

$$+ (a_2 + a_1 \cos \Delta\psi) \frac{\partial a_2(\alpha)}{\partial \alpha}]$$

$$- (\beta_g^{-1} - \dot{\xi}/c) \, c\Delta\omega \, a_1 a_2 \sin \Delta\psi\},$$

where $\dot{\xi} = \partial\xi(z_o,\tau)/\partial\tau$, $\alpha = z_o + \xi - v_g\tau$ and $\Delta\psi(z_o,\tau) = \Delta k\{z_o + \xi(z_o,\tau)\}$ $- \Delta\omega\tau + \Delta\phi$.

The imposed laser field and the applied transverse magnetic field modify the plasma frequency and hence we define an effective plasma frequency

$$\omega_s = (\frac{\omega_p^2}{\gamma_{\perp o}} + \frac{\Omega^2}{\gamma_{\perp o}^2})^{1/2}, \tag{15}$$

where

$$\gamma_{\perp o} = [1 + \frac{1}{2}(a_{1,max}^2 + a_{2,max}^2)]^{1/2}. \tag{16}$$

The effective plasma frequency, ω_s, is the relativistic upper hybrid frequency. An increase in the transverse oscillations results in a decrease in the velocity of the axial oscillation, which in turn leads to an effective reduction in the plasma frequency. On the other hand, the transverse magnetic field results in an increase in the effective plasma frequency.

C. Normalized Plasma Wave Equation

To further study the dynamics of the plasma oscillations, we normalize the parameters in the following manner,

$$T = \Delta\omega\tau, \tag{17}$$

$$E = \frac{\Delta k}{\omega_p^2} \frac{|e|}{m_o} E_z = \Delta k\xi,$$

9

$$Z_o = \Delta k z_o,$$

$$f = \Delta\omega/\omega_s,$$

and
$$G = (\Omega^2/\gamma_{\perp o}^2)\ (\omega_p^2/\gamma_{\perp o})^{-1}.$$

The evolution of the plasma oscillation is now given by

$$\ddot{E} + \frac{1}{f^2(1+G)}(1 - \beta_g^2\dot{E}^2)\frac{\gamma_{\perp o}}{\gamma_\perp}\lfloor(1-\beta_g^2\dot{E}^2)^{1/2} + G\frac{\gamma_{\perp o}}{\gamma_\perp}\rfloor E \qquad (18)$$

$$= -\frac{(1-\beta_g^2\dot{E}^2)(1-\beta_g^2\dot{E})}{2\beta_g^2\gamma_\perp^2}\lfloor(a_1 + a_2\cos\Delta\psi)\frac{\partial a_1(\alpha)}{\partial\alpha}$$

$$+ (a_2 + a_1\cos\Delta\psi)\frac{\partial a_2(\alpha)}{\partial\alpha} - a_1 a_2\sin\Delta\psi\rfloor,$$

where

$$\gamma_\perp = \lfloor 1 + \frac{\beta_g^2}{f^2}\frac{G}{1+G}\gamma_{\perp o}^2 E^2 + \frac{1}{2}(a_1^2 + a_2^2) + a_1 a_2\cos\Delta\psi\rfloor^{1/2}, \qquad (19)$$

$$\Delta\psi = E - T + Z_o + \Delta\phi, \qquad (20)$$

$\alpha = Z_o + E - T$ and $\dot{E} = \partial E(Z_o,T)/\partial T$. The total relativistic mass factor associated with the plasma motion becomes

$$\gamma(Z_o,T) = \gamma_\perp(1 - \beta_g^{-2}\dot{E}^2)^{-1/2}. \qquad (21)$$

Since the plasma oscillation amplitude is single valued, our model is valid prior to electron trapping, i.e., trajectory crossing. Trajectory crossing occurs when the amplitude $|E|$ is approximately unity.

The equation of motion described by Eq. (18) is fully relativistic in both the axial and transverse directions and permits us to model laser pulses with a beat frequency other than the plasma frequency. Also by varying the parameter G associated with the transverse magnetic field we can also model the surfatron configuration.

III. Analytical Theory in the Weak Laser Field

In this section we derive the scaling laws appropriate for weak laser fields, i.e., electron transverse motion is mildly relativistic. Here, we consider the case where the two laser powers are constant in time and define the small parameter

$$\epsilon = \frac{a_1 a_2}{1 + \frac{1}{2}(a_1^2 + a_2^2)}, \tag{22}$$

where the denominator of ϵ, is associated with the relativistic motion in the transverse direction, $\gamma_{\perp 0}^2$. When $a_1 = a_2$, ϵ is proportional to the laser powers.

Assuming E to be a slowly varying function of time, it can be represented in the form

$$E(Z_0, T) = \Delta E(T) \sin \left[Z_0 - T + \theta(T) + \Delta\phi \right], \tag{23}$$

where $\Delta E(T)$ and $\theta(T)$ are slowly varying functions of time compared to the plasma oscillation period. Furthermore, we assume that ω_1, $\omega_2 \gg \omega_p$, so that $\Delta\omega/c\Delta k \simeq 1$.

A. Small Parameter Expansion

Expanding Eq. (18) in terms of the small parameters ϵ and E , we obtain the following equation for E,

$$\ddot{E} + \frac{1}{f^2} E = \frac{\epsilon}{2} \sin \Delta\psi + F \tag{24}$$

where

$$F(Z_0, T) = \left[\frac{1}{f^2} - \frac{(1-G)}{f^2} (1 - \frac{3}{2} E^2)(1 - \frac{\epsilon}{2} \cos\Delta\psi) - \frac{G}{f^2} (1 - \epsilon \cos \Delta\psi) \right] E$$

12

$$- \frac{\varepsilon}{2} \left\lfloor \dot{E} + \varepsilon \cos \Delta\psi \right\rfloor \sin \Delta\psi,$$

$\Delta\psi = \Delta E(T) \sin \Phi(Z_o, T) - T + Z_o + \Delta\phi$, and $\Phi = Z_o - T + \Delta\phi + \theta(T)$. Using the identities,

$$\sin \Delta\psi = \sum_{\ell=-\infty}^{\infty} J_\ell(\Delta E) \sin\{(\ell+1)\Phi - \theta\}, \tag{25a}$$

$$\cos \Delta\psi = \sum_{\ell=-\infty}^{\infty} J_\ell(\Delta E) \cos\{(\ell+1)\Phi - \theta\}, \tag{25b}$$

and keeping only terms that are proportional to $\sin \Phi$ and $\cos \Phi$, we obtain

$$(1 - \frac{1}{f^2} - 2 \frac{d\theta}{dT}) \Delta E \sin \Phi + 2 \frac{d\Delta E}{dT} \cos \Phi = - \frac{\varepsilon}{2} J_o(\Delta E) \sin(\Phi - \theta) - F, \tag{26}$$

where

$$F = \left\{ \frac{3}{8} \frac{\Delta E^3}{f^2} - \frac{\varepsilon}{4} \Delta E \left\lfloor \frac{3(1 - 3G)}{f^2} + 1 \right\rfloor J_1(\Delta E) \cos \theta + \frac{\varepsilon^2}{4} J_1(2\Delta E) \cos 2\theta \right\} \sin \Phi$$

$$+ \left\{ \frac{\varepsilon\Delta E}{4} \left\lfloor \frac{(1 - 3G)}{f^2} + 1 \right\rfloor J_1(\Delta E) \sin \theta - \frac{\varepsilon^2}{4} J_1(2\Delta E) \sin 2\theta \right\} \cos \Phi.$$

Using the small parameter expansions for the Bessel functions, i.e., $J_o(x) \approx 1 - x^2/4$ and $J_1(x) \approx x/2$, Eq. (26) becomes

$$2 \frac{d\theta}{dT} \Delta E \sin \Phi - 2 \frac{d\Delta E}{dT} \cos \Phi = \Delta E(1 - \frac{1}{f^2}) \sin \Phi \tag{27}$$

$$+ \frac{\varepsilon}{2} (1 - \frac{\Delta E^2}{4})[\sin \Phi \cos \theta - \cos \Phi \sin \theta] + F,$$

13

where

$$F = [\frac{3}{8} \frac{\Delta E^3}{f^2} - \frac{\epsilon}{8} \frac{\Delta E^2}{f^2} (2 - 9G) \cos \theta + \frac{\epsilon^2}{4} \Delta E \cos(2\theta)] \sin \phi$$

$$+ [\frac{\epsilon}{8} \frac{\Delta E^2}{f^2} (2 - 3G) \sin \theta - \frac{\epsilon^2}{4} \Delta E \sin(2\theta)] \cos \phi .$$

Separating the terms proportional to $\sin \phi$ and $\cos \phi$, we obtain two simultaneous coupled equations for the amplitude and phase variation of the excited plasma wave,

$$\frac{d\Delta E}{dT} = \epsilon [\frac{1}{4} - \frac{\Delta E^2}{16}(1 + \frac{2}{f^2} - \frac{3G}{f^2})] \sin \theta + \frac{\epsilon^2 \Delta E}{8} \sin 2\theta, \tag{28a}$$

$$\Delta E \frac{d\theta}{dT} = \frac{\Delta E}{2} \frac{f^2 - 1}{f^2} + \frac{3}{16} \frac{\Delta E^3}{f^2} + \epsilon [\frac{1}{4} - \frac{\Delta E^2}{16}(\frac{2}{f^2} + 1 - \frac{9G}{f^2})] \cos \theta + \frac{\epsilon^2}{8} \Delta E \cos 2\theta .$$

$$\tag{28b}$$

B. Constant of Motion

Analytical expressions for ΔE and phase velocity v_{ph} of the plasma wave can be obtained by assuming $1 \gg \Delta E \gg \epsilon$. It will be shown later that this assumption is well founded. Neglecting terms proportional to $\epsilon \Delta E^2$ and $\epsilon^2 \Delta E$ in Eq. (28) we obtain,

$$\frac{d\Delta E}{dT} \approx \frac{\epsilon}{4} \sin \theta, \tag{29a}$$

$$\Delta E \frac{d\theta}{dT} \approx \frac{\Delta E}{2} \frac{f^2 - 1}{f^2} + \frac{\epsilon}{4} \cos \theta + \frac{3}{16} \frac{\Delta E^3}{f^2} . \tag{29b}$$

Multiplying Eq. (29a) by $\cos \theta$ and Eq. (29b) by $\sin \theta$ and adding the two

equations yield

$$\frac{d}{dT} (\Delta E \cos \theta) = \left\{ -\frac{\Delta E}{2} \frac{(f^2 - 1)}{f^2} - \frac{3}{16} \frac{\Delta E^3}{f^2} \right\} \sin \theta. \tag{30}$$

Using (29a) and (30), the following constant of the motion is obtained

$$\Delta E \left\{ \Delta E^3 + \frac{16}{3} (f^2 - 1) \Delta E + \frac{16}{3} f^2 \varepsilon \cos \theta \right\} = C, \tag{31}$$

where $C = 0$, since initially $\Delta E = 0$.

Employing (30), Eqs. (29a) and (29b) become

$$\frac{d\Delta E}{dT} = \frac{\varepsilon}{4} \sin \theta, \tag{32a}$$

and

$$\frac{d\theta}{dT} = \frac{1}{4 f^2} (f^2 - 1 + \frac{9}{16} \Delta E^2), \tag{32b}$$

where the initial conditions are, $\Delta E = 0$, and $\theta = \pi/2$. An alternate way to solve ΔE and θ in time is outlined in Appendix A. At exact resonance $f = 1$ and nonrelativistic motion in the transverse direction, i.e., $\gamma_{\perp o}^2 \simeq 1$ and $\varepsilon \simeq a_1 a_2$, the expressions (32a,b) agree with that of Rosenbluth and Liu.[24]

C. Analytical Results

We obtain analytical results for the start-up as well as the saturated regimes of the plasma wave. The plasma wave initially grows linearly in time, i.e., the initial amplitude of E_z in c.g.s. units is proportional to Γt, where

$$\Gamma = \frac{\beta_g}{4} \frac{m_o c}{|e|} \omega_p^2 \varepsilon. \tag{33}$$

15

The most interesting results are associated with the saturated regime. In the remainder of this section, we obtain maximum accelerating electric fields, the appropriate laser beat frequencies, the corresponding phase velocities and the plasma wave profiles.

The amplitude of the electric field is proportional to a real root of the cubic polynomial (31). The roots are:

$$\Delta E = A + B, \qquad -\frac{A + B}{2} + \frac{A - B}{2} \sqrt{-3}, \qquad -\frac{A + B}{2} - \frac{A - B}{2} \sqrt{-3}, \qquad (34)$$

where $A = (- b/2 + h)^{1/3}$, $B = (- b/2 - h)^{1/3}$, $h = (b^2/4 + a^3/27)^{1/2}$, $a = 16/3 \, (f^2 - 1)$ and $b = 16/3 \, f^2 \varepsilon \cos \theta$. For $h > 0$, there is one real root given by $\Delta E = A + B$. When $h < 0$, there are three real roots, and numerical results show that the relevant ΔE corresponds to the smallest real root. At $h = 0$, ΔE undergoes a discontinuity.

For a given laser power parameter ε, the maximum ΔE occurs at $h = 0$ and $\cos \theta = - 1$, giving

$$\Delta E_{max} = 4 \, (\frac{\varepsilon}{3})^{1/3}, \qquad (35)$$

where ε is defined in Eq. (22). The actual maximum field in c.g.s. units is

$$E_{z,max} = 4(\frac{\omega_p^2}{\Delta\omega}) \, \beta_g \, \frac{m_o c}{|e|} \, (\frac{\varepsilon}{3})^{1/3}. \qquad (36)$$

As the laser power is increased, relativistic effects on the electron motion become significant. These relativistic effects cause the accelerating field to maximize at a laser beat frequency which is less than the effective plasma frequency. For example when the beat frequency is exactly equal to the

16

effective plasma frequency, i.e., $f = 1$, the maximum normalized field is

$$\Delta E = (\frac{16}{3} \varepsilon)^{1/3} < \Delta E_{max}. \qquad (37)$$

It can be shown that the electric field maximizes to the value in Eq. (35), when the normalized laser beat frequency is

$$f_{opt} = 1 - \frac{1}{2} (\frac{9}{8} \varepsilon)^{2/3}, \qquad (38)$$

which corresponds to a laser beat frequency in c.g.s. units given by

$$\Delta\omega_{opt} = \omega_s (1 - 0.54 \varepsilon^{2/3}). \qquad (39)$$

During the acceleration process the injected electrons must be nearly synchronized with the phase velocity of the plasma wave. To obtain the phase velocity, we follow a null in the plasma wave. We find that the phase velocity of the plasma wave and the associated relativistic mass factor are

$$v_{ph} = v_g (1 - d\theta/dT), \qquad (40a)$$

and

$$\gamma_{ph} = \gamma_g (1 + 2 \gamma_g^2 d\theta/dT)^{-1/2}, \qquad (40b)$$

where $d\theta/dT$ is given by (32b) and $\gamma_g = [1 - (v_g/c)^2]^{-1/2}$. As the amplitude of the plasma wave becomes larger, the phase velocity of the plasma wave decreases. The phase velocity of the plasma wave at the maximum electric

17

field amplitude is a minimum and given by

$$v_{ph,min} = v_g (1 - 1.89 \, \varepsilon^{2/3}).$$ (41)

The time it takes the amplitude of the plasma wave to reach the first peak is called the plasma build-up time and in normalized units is given by

$$\tilde{T}(f,\varepsilon) = 4 \int_{\pi/2}^{\pi} \frac{d\theta}{f^2 - 1 + (9/16)\Delta E^2},$$ (42)

where ΔE is expressed in terms of θ in Eq. (34). The equation above can be integrated at exact resonance, i.e., $f = 1$. Using the fact that $\Delta E = (-\frac{16}{3} \varepsilon \cos\theta)^{1/3}$ at $f = 1$, we can write

$$\tilde{T}(1,\varepsilon) = \frac{64}{9} (\frac{3}{16})^{2/3} \varepsilon^{-2/3} \int_{\pi/2}^{\pi} \frac{d\theta}{(- \cos\theta)^{2/3}}.$$ (43)

Evaluating the integral in (43), we obtain

$$\tilde{T}(1,\varepsilon) = \frac{32}{9} (\frac{3}{16})^{2/3} \frac{\Gamma(1/6)\Gamma(1/2)}{\Gamma(2/3)} \varepsilon^{-2/3} = 8.48\varepsilon^{-2/3}.$$ (44)

Taking $\varepsilon = 0.01$ as an example, the plasma build-up time at exact resonance is 29.1 plasma periods, i.e., $\tilde{T}(1,0.01) = 29.1(2\pi)$. For $\varepsilon = 0.1$, the plasma build-up time is reduced to only 6.3 plasma periods. The plasma build-up time shortens as laser power parameter ε increases.

Finally, we discuss the effect of unequal applied laser pulse powers on the plasma wave dynamics. Suppose a given value of ε is desired, the total power required for the laser is at a minimum when $a_1 = a_2 = a$ where

18

$a = (\frac{\varepsilon}{1 - \varepsilon})^{1/2}$. The expression for a_2 given a_1 and ε is

$$a_2 = \frac{a_1}{\varepsilon} - \{\frac{a_1^2}{\varepsilon} - (2 + a_1^2)\}^{1/2}. \tag{45}$$

The range for a_1 given ε is

$$a_{min} = (\frac{2\varepsilon^2}{1 - \varepsilon^2})^{1/2} < a_1 < a_{max} = (\frac{2}{1 - \varepsilon^2})^{1/2}. \tag{46}$$

A plot of $a_1^2 + a_2^2$ is given in Fig. 2 for $\varepsilon = 0.1$. The use of unequal laser powers can be advantageous in controlling the value of the parameter ε.

IV. Numerical Results

Numerical examples are given for the complete nonlinear and fully relativistic equations obtained in Section II, and these results are compared to the analytical results obtained in Section III in the weak laser field limit, i.e., $\epsilon \ll 1$.

Equations (32a,b) were numerically solved in order to verify our approximation $|\Delta E| \gg \epsilon$ used in deriving the constant of motion. Figure 3 is a plot of $|\Delta E|$ as a function of time for the parameters, $\epsilon = 0.01$, $G = 0$ and three different normalized frequencies: $f = 0.96$, $f = 0.98$ and $f = 1.0$. The curves show that the approximation, $|\Delta E| \gg \epsilon$, is indeed well-satisfied. The curves for $|\Delta E|$ in Fig. 3 are periodic in time and show that the plasma wave periodically exchanges its energy with the laser field. The plasma build-up time is longest when the frequency is f_{opt}, and is 29 plasma periods with $f = 1$ and $\epsilon = 0.01$, agreeing with the calculations in Section III. C.

Figure 4 is a plot of the amplitude of E as a function of time for the complete equations (18-20), with the same parameters as used in Fig. 3. The laser power was built-up gradually over three periods of the laser beat frequency. We used $\beta_g = 0.9999$ for the purpose of comparing with analytical results. In this case, the amplitudes of the plasma electric fields are only slightly changed, showing that the analytical equations are excellent in the small ϵ limit.

In Fig. 5, the phase velocities given by the analytical results (solid curve) are compared to the numerical values (dashed curve) for $\epsilon = 0.01$ and $f = 0.98$. The shift of the two curves is due to the three periods of laser build-up time in the numerical calculation. The phase velocity v_{ph} is at a local minimum when $|\Delta E|$ is maximum and decreases as ΔE increases.

The plots of the numerically calculated peak amplitude of E (dashed curve) and the analytical expression $\Delta E_{max} = 4(\epsilon/3)^{1/3}$ (solid curve) are

20

plotted as a function of $\varepsilon^{1/3}$ in Fig. 6. The plots of the normalized laser beat frequency f (dashed curve), at which the largest accelerating electric field is numerically obtained and the analytical expression for f_{opt} (solid curve) are shown in Fig. 7 as a function of $\varepsilon^{2/3}$.

The normalized peak amplitudes of the accelerating electric field for $\varepsilon = 0.01$, 0.04 and 0.16 in the frequency range $0.8 < f < 1.1$ are given in Fig. 8. The phase velocities associated with the peak amplitude are plotted in Fig. 9. The dashed curves are the numerical results obtained from the complete nonlinear and fully relativistic equations (18-20), while solid curves are the analytical results obtained from Eq. (34). The agreement for small ε is excellent.

We note that the analytical solutions for the amplitude of the plasma wave and the phase velocity have discontinuities at f_{opt}. For $f > f_{opt}$, ΔE has one real root and the phase velocity associated with the peak electric field is less than the speed of light. For $f < f_{opt}$, ΔE has three real roots. The smallest value of the root is closest to the numerical result. For $f < f_{opt}$, the phase velocity associated with the peak electric field is generally greater than the speed of light.

In the region marked by (= = = = =) in Fig. 8, the analysis is not applicable because of particle mixing. Here, the large amplitude oscillations cause the electrons to become relativistic resulting in wave steepening,[20,24] which phenomenon is illustrated in Fig. 10. Two curves of the normalized electric field at two instants of time are plotted for one wavelength of the laser beat wave with parameters $\varepsilon = 0.16$ and $f = 0.925$, the point is marked by (*) on Fig. 8. The curve with the circular dots showing wave steepening, is the normalized electric field just before wave breaking. On the other hand, the wave profile is almost sinusoidal when the amplitude of the electric field

is small, i.e., $|\Delta E| \ll 1$, as illustrated by the curve with the crosses in Fig. 10. As $|\Delta E|$ becomes larger than 1.1, the electric field in our representation becomes multivalued and the Lagrangian model breaks down. Since the electric field produced by a turbulent plasma is unlikely to be desirable for acceleration of electrons, the upper limit for $|\Delta E|$ is $\Delta E_{Lim} = 1.1$. The minimum ε necessary to obtain ΔE_{Lim} is approximately $\varepsilon_{min} = 0.06$.

To illustrate the relativistic phenomenon, Fig. 11 shows a plot of $\gamma_z = (1 - (v_z/c)^2)^{-1/2}$ for one wavelength of the laser beat wave for the same parameters and at the same instants in time as Fig. 10.

Numerically calculated time evolution of the electric field and the corresponding phase velocity for $f = 0.925$ are plotted in Figs. 12 and 13 respectively, where ε is adiabatically increased from 0 to 0.16 in three plasma periods.

Since the saturated oscillatory electric field amplitudes and phase velocities are not desirable for accelerating electrons, the laser pulse duration should be chosen to equal the plasma build-up time. After the laser pulses pass through the plasma, the plasma wave will continue to oscillate until disrupted by various instabilities. Figure 14 plots the temporal profiles of the normalized stimulated electric field amplitude (solid curve) for $f = 0.925$ and a short laser beat wave pulse $\varepsilon(t)$ (dashed curve). The corresponding phase velocity is shown in Fig. 15. After the laser pulse passed, the amplitude and the phase velocity of the plasma oscillation remained roughly constant.

Next, we examined the effect of the perpendicular magnetic field on the plasma oscillation in the surfatron configuration. An imposed transverse magnetic field can increase the total electron energy by maintaining synchronism while accelerating the electrons in the transverse direction.[22]

The analytical calculation shows that the transverse magnetic field has a higher order effect on the plasma dynamics. The numerical result of the peak electric field and the corresponding phase velocity are plotted as a function of G for $\epsilon = 0.16$ and $f = 0.925$ in Fig. 16, and results changed little for $0 \leq G \leq 1$. The imposed transverse magnetic field increases the effective plasma frequency, but has little effect on the dynamics of the plasma wave.

V. Summary

We have obtained nonlinear, fully relativistic results for the plasma waves excited by the beating of two laser beams. We found that the effective plasma frequency is a function of the laser power as well as the imposed transverse magnetic field in the surfatron configuration. In the ideal situation analyzed here, the amplitude of plasma waves becomes oscillatory. Since it is desirable to maintain the accelerating electric field at the largest value, the laser pulse duration should be approximately equal to the plasma wave build-up time.

In the weak laser power limit, we obtained analytical results for the saturated plasma wave for a range of frequencies around the effective plasma frequency. As the laser power increases, the maximum amplitude of the plasma electric field increases as $\varepsilon^{1/3}$, confirming the previous work of Rosenbluth and Liu[24] at exact resonance when the transverse motion is nonrelativistic, i.e., $\gamma_{\perp o} = 1$, and the corresponding phase velocity decreases, i.e., $v_g - v_{ph}$ scales as $\varepsilon^{2/3}$. The maximum accelerating field is achieved when the laser beat frequency is less than the effective plasma frequency. The difference between the effective plasma frequency and the optimal laser beat frequency is proportional to $\varepsilon^{2/3}$. The plasma build-up time is proportional to $\varepsilon^{-2/3}$.

Given a plasma density, the desirable range of normalized laser beat frequency for growth of large amplitude plasma waves is small, i.e., $1.05 \gtrsim f \gtrsim f_{opt}$. If the laser beat frequency is given, this condition can be translated to plasma density requirements. Defining $n_o = \Delta n + n_{f=1}$, where $n_{f=1}$ is the ambient plasma density that will provide exact resonance at $f=1$, i.e., $\omega_s(n_{f=1}) = (\omega_{po}^2/\gamma_{\perp o} + \Omega^2/\gamma_{\perp o}^2)^{1/2} = \Delta\omega$, where $\omega_{po} = (4\pi|e|^2 n_{f=1}/m_o)^{1/2}$. The density criteria for stimulating large amplitude plasma waves is

$$- 0.1 \; (1 + G_o) \lesssim \frac{\Delta n}{n_{f=1}} \leq 1.1 \; \epsilon^{2/3} \; (1 + G_o),$$ (47)

where $G_o = (\Omega^2/\gamma_{1o}^2)(\omega_{po}^2/\gamma_{1o})^{-1}$. We now consider two examples of plasma density variation requirements without imposed transverse magnetic field, i.e., $G_o = 0$. The largest tolerable plasma density variation is about 25% for $\epsilon = 0.06$. The tolerable density variation is reduced to 15% for $\epsilon = 0.01$. The application of transverse magnetic field B_o in the surfatron configuration can increase the allowable density fluctuation limit by a factor $(1 + G_o)$. In an experimental situation, B_o, not only overcomes the problem of desynchronization, but allows more flexibility in the tuning of plasma density.

A comparison of the numerical results from the complete equations with the simple analytical results for the weak laser power limit is excellent for $\epsilon \ll 0.1$, and is in fair agreement for larger ϵ. Numerical results show that the largest amplitude for the accelerating electric field in cgs units without electrons overtaking each other is

$$|E_z| \simeq (\frac{\omega_p^2}{\Delta\omega}) \; \beta_g \; \frac{m_o c}{|e|} \; .$$

The laser power required to reach this value without wave breaking is $\epsilon \sim 0.06$.

For the purpose of accelerating electrons, it is desirable not only to have the largest accelerating electric field but also have v_{ph}/c less than but close to unity. Instead, we find that as the amplitude of plasma waves get larger, the corresponding phase velocities become smaller. An applied transverse magnetic field can overcome the problem of desynchronization of the accelerating electrons in the accelerative electric field. Since the

25

transverse magnetic field only modifies the effective plasma frequency, but has little effect on the plasma dynamics, the surfatron configuration may be the desirable way to operate the laser beat wave accelerator.

Finally, we would like to point out that the laser plasma interaction contains a rich source of instabilities, many of which may be detrimental for the formation of the large amplitude plasma waves studied in this paper for the laser beat wave accelerating scheme. Some of the processes[19] that have large growth rates are three-wave forward Raman scattering, four-wave forward Raman scattering, and processes associated with background ions. Other areas requiring investigations are the effects of the transverse Weibel instability induced by energy anisotropy, the influence of kinetic effects, self-focusing of laser radiation and filamentation. Detailed studies of them are necessary to evaluate feasibility of the long term goals of the laser beat wave accelerating scheme.

Acknowledgments

References

1. *Laser Acceleration of Particles*, AIP Conf. Proc. No. 91, Ed. by Paul J. Channell, American Institute of Physics, New York, 1982.

2. Challenge of Ultra-High Energies: Ultimate Limits, Possible Directions of Technology, an Approach to Collective Acceleration. ECFA Report 83/68 published by Rutherford Appleton Laboratory (1983).

3. H. Motz, Contemp. Phys. $\underline{20}$, 547 (1979).

4. P. Sprangle and Cha-Mei Tang, IEEE Trans. on Nuclear Sci., $\underline{NS\text{-}28}$, 3346 (1981).

5. C. Pellegrini, Ref. 1 p. 138 and Ref. 2 p. 249.

6. R. B. Palmer, Ref. 1 p. 179 and Ref. 2 p. 267.

7. R. H. Pantell and T. I. Smith, Appl. Phys. Lett., $\underline{40}$, 753 (1982).

8. J. R. Fontana and R. H. Pantell, J. Appl. Phys., $\underline{54}$, 4285 (1983).

9. A. A. Kolomenskii and A. N. Lebedev, Soviet Physics, Dokl., $\underline{7}$, 745 (1963).

10. P. Sprangle, L. Vlahos and C. M. Tang, IEEE Trans. on Nucl. Sci., $\underline{NS\text{-}30}$, 3177 (1983).

11. A. M. Sessler, Ref. 1 p. 154.

12. T. Tajima and J. M. Dawson, Phys. Rev. Lett. $\underline{43}$, 267 (1979).

13. T. Tajima and J. M. Dawson, IEEE Trans. Nucl. Sci. $\underline{NS\text{-}26}$, 4188 (1979).

14. T. Tajima and J. M. Dawson, IEEE Trans. Nucl. Sci. $\underline{NS\text{-}28}$, 3416 (1981).

15. C. Joshi, T. Tajima, J. M. Dawson, H. A. Baldis and N. A. Ebrahim, Phys. Rev. Lett. $\underline{47}$, 1285 (1981).

16. M. Ashour-Abdalla, J. N. Leboeuf, T. Tajima, J. M. Dawson and C. F. Kennel, Phys. Rev. A $\underline{23}$, 1906 (1981).

17. D. J. Sullivan and B. B. Godfrey, IEEE Trans. Nucl. Sci. $\underline{NS\text{-}28}$, 3395 (1981).

18. J. D. Lawson, Rutherford Appleton Laboratory, Report RL-83-057, 1983. PB83-256297

19. R. Bingham, private communications (1983).

20. R. J. Noble, submitted to the Proc. of the 12th Intl. Conf. on High Energy Acc., Fermi National Lab., 11-16 Aug (1983).

21. B. I. Cohen, Lawrence Livermore National Lab., Report UCRL-89871, 1983.

22. T. Katsouleas and J. M. Dawson, Phys. Rev. Lett. $\underline{51}$, 392 (1983).

23. R. C. Davidson, Methods in Nonlinear Plasma Theory, Academic Press, NY (1972).

24. M. N. Rosenbluth and C. S. Liu, Phys. Rev. Lett. $\underline{29}$, 701 (1972).

Appendix A: Alternative View of Equations (32a,b)

The simplified equations in (32a,b) can be written in the form

$$\frac{dx}{dT} = \frac{1}{2\,f^2} \left[1 - f^2 - \frac{3}{8} (x^2 + y^2) \right] y, \qquad\qquad (A-1)$$

$$\frac{dy}{dT} = \frac{\epsilon}{4} - \frac{1}{2\,f^2} \left[1 - f^2 - \frac{3}{8} (x^2 + y^2) \right] x, \qquad\qquad (A-2)$$

where $x = \Delta E \cos \theta$, $y = \Delta E \sin \theta$ and the initial conditions are $x = y = 0$ at
$T = 0$.   The amplitude and the phase of the electron displacement are

$$\Delta E = (x^2 + y^2)^{1/2} \quad \text{and} \quad \theta = \tan^{-1} \left(\frac{y}{x} \right). \qquad\qquad (A-3a,b)$$

Figure 17 is a plot of x and y for $\epsilon = 0.01$ and three different normalized laser
beat frequencies: $f = 0.96$, 0.98 and 1.0.   For $f > f_{opt}$, the enclosed area is to
the left of $x = 0$, and to the right of $x = 0$ for $f < f_{opt}$.

30

High Energy
Electrons

Plasma

$\Delta\omega = \omega_1 - \omega_2 \simeq \omega_P$

B_0

Applield Transverse Magnetic Field

Lasers $\begin{cases} \omega_1 \\ \omega_2 \end{cases}$

Low Energy
Electrons
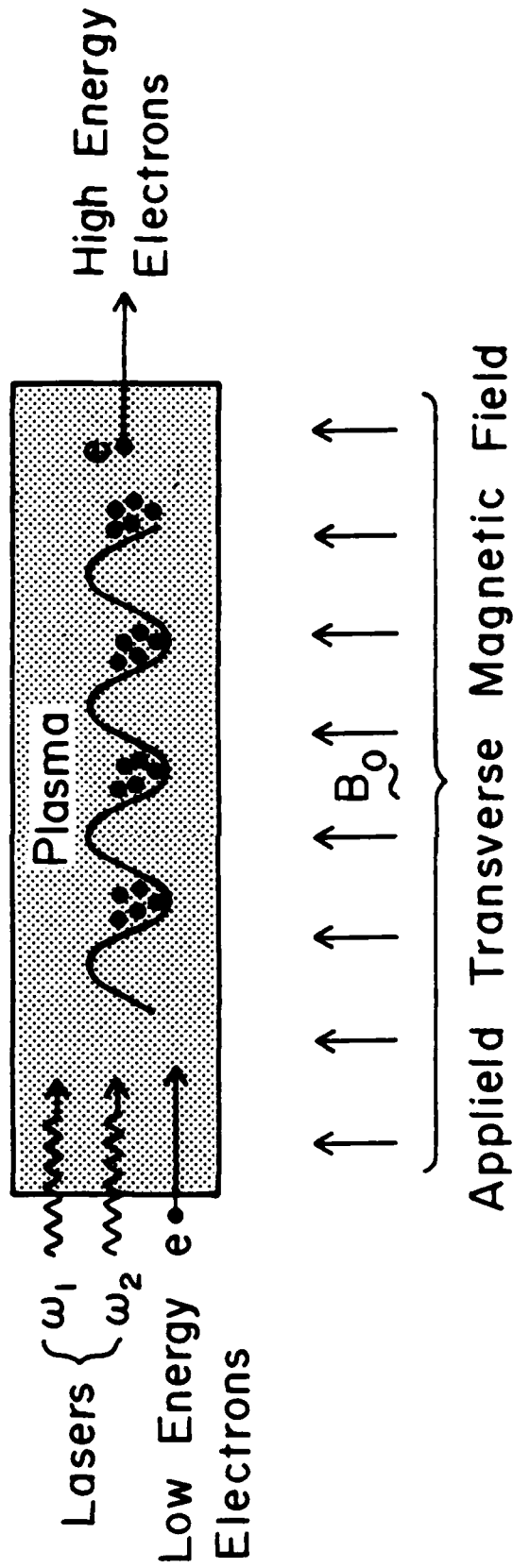
Fig. 1   The schematic of electron acceleration by plasma waves excited by

two lasers with a beat frequency approximately equal to the plasma

frequency.
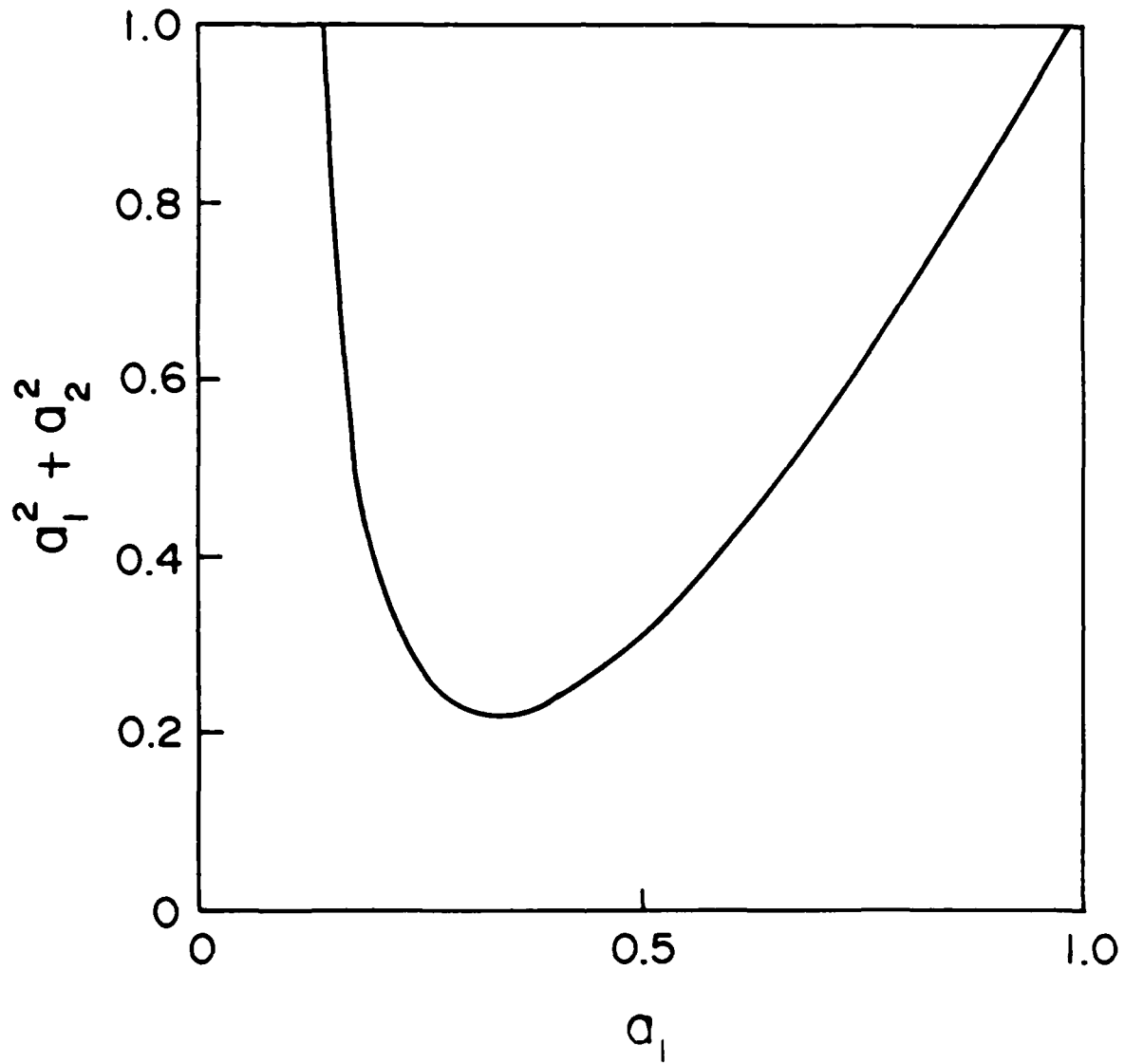
Fig. 2   Plot of $a_1^2 + a_2^2$ as a function of a_1 for $\varepsilon = 0.1$.
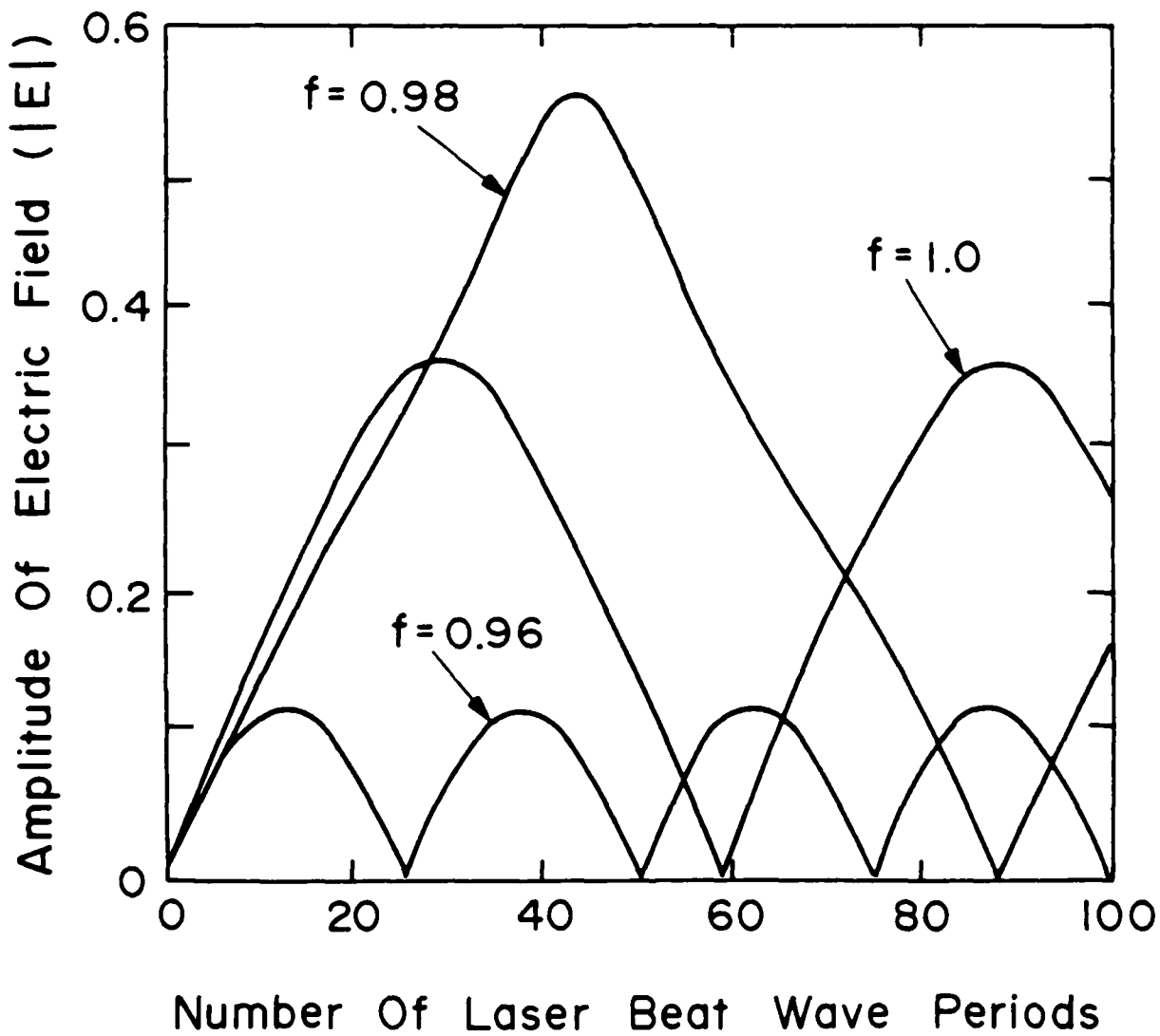
Fig. 3   Plot of $|\Delta E|$ as a function of number of laser beat wave periods

for $\epsilon = 0.01$, $G = 0$ and three different beat frequency parameters

$f = 0.96$, 0.98 and 1.0.

33
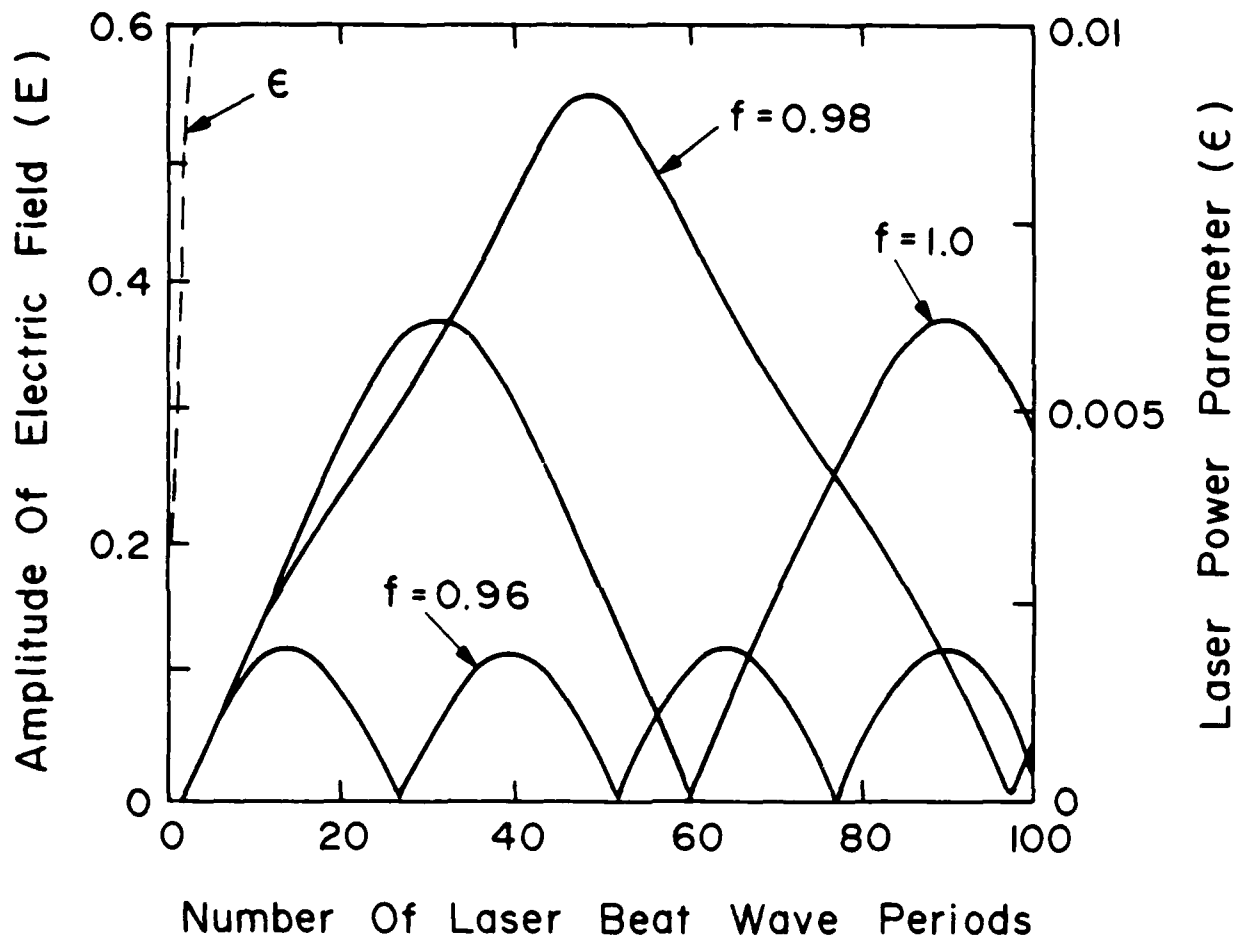
Fig. 4 Normalized amplitude of the accelerating electric field
E as a function of the number of laser beat wave periods obtained
with the fully relativistic equations for laser powers built-up over
three laser periods.
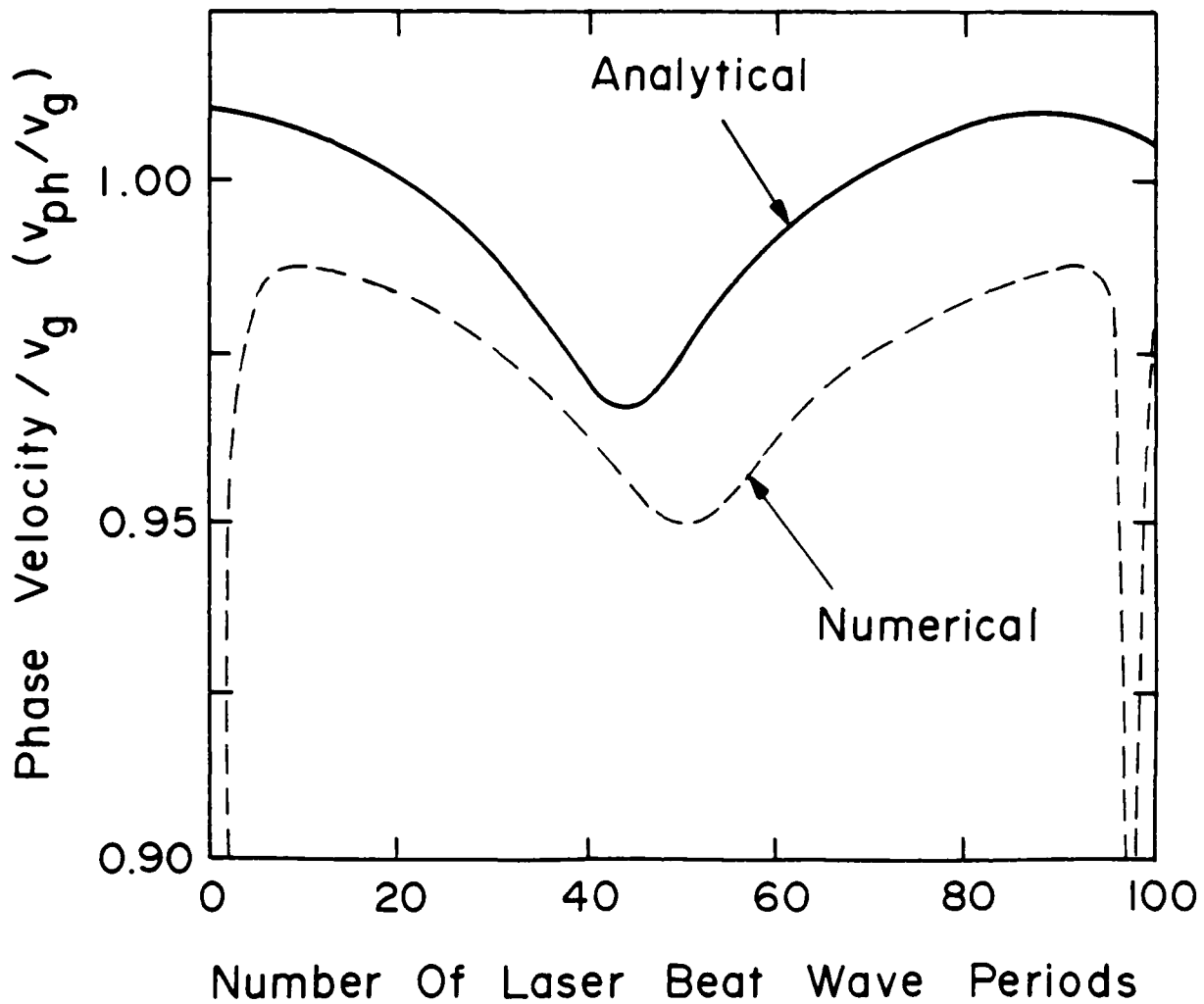
Fig. 5   Phase velocities obtained from the simplified equations (solid curve)
and numerically obtained from the fully relativistic nonlinear
equations (dashed curve) for $\epsilon = 0.01$, $G = 0$ and $f = 0.98$.

35
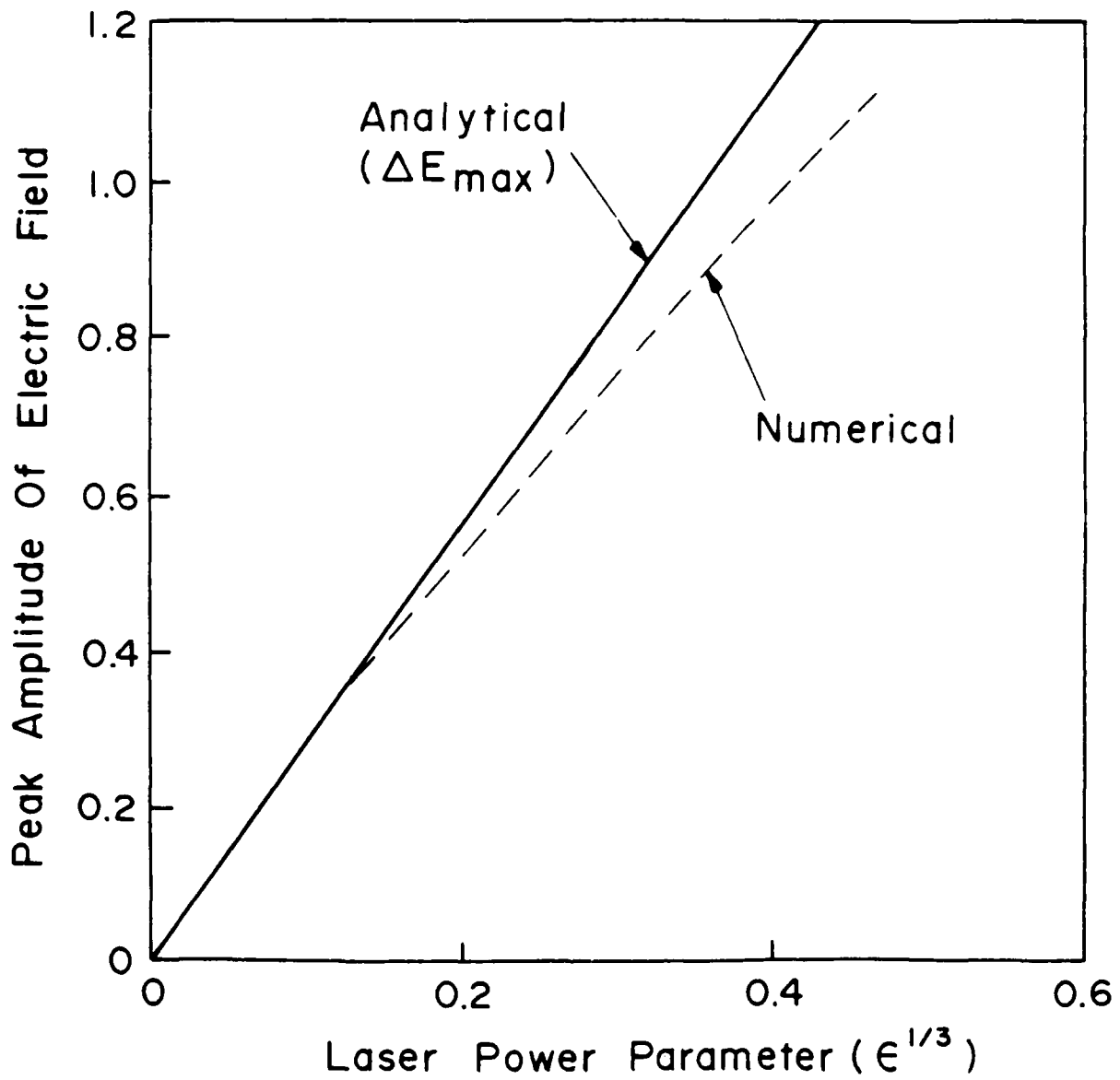
Fig. 6   Comparison of ΔE_{max} based on the analytical result (solid curve), and

the peak amplitude of E numerically obtained from the fully

relativistic nonlinear equations (dashed curves).
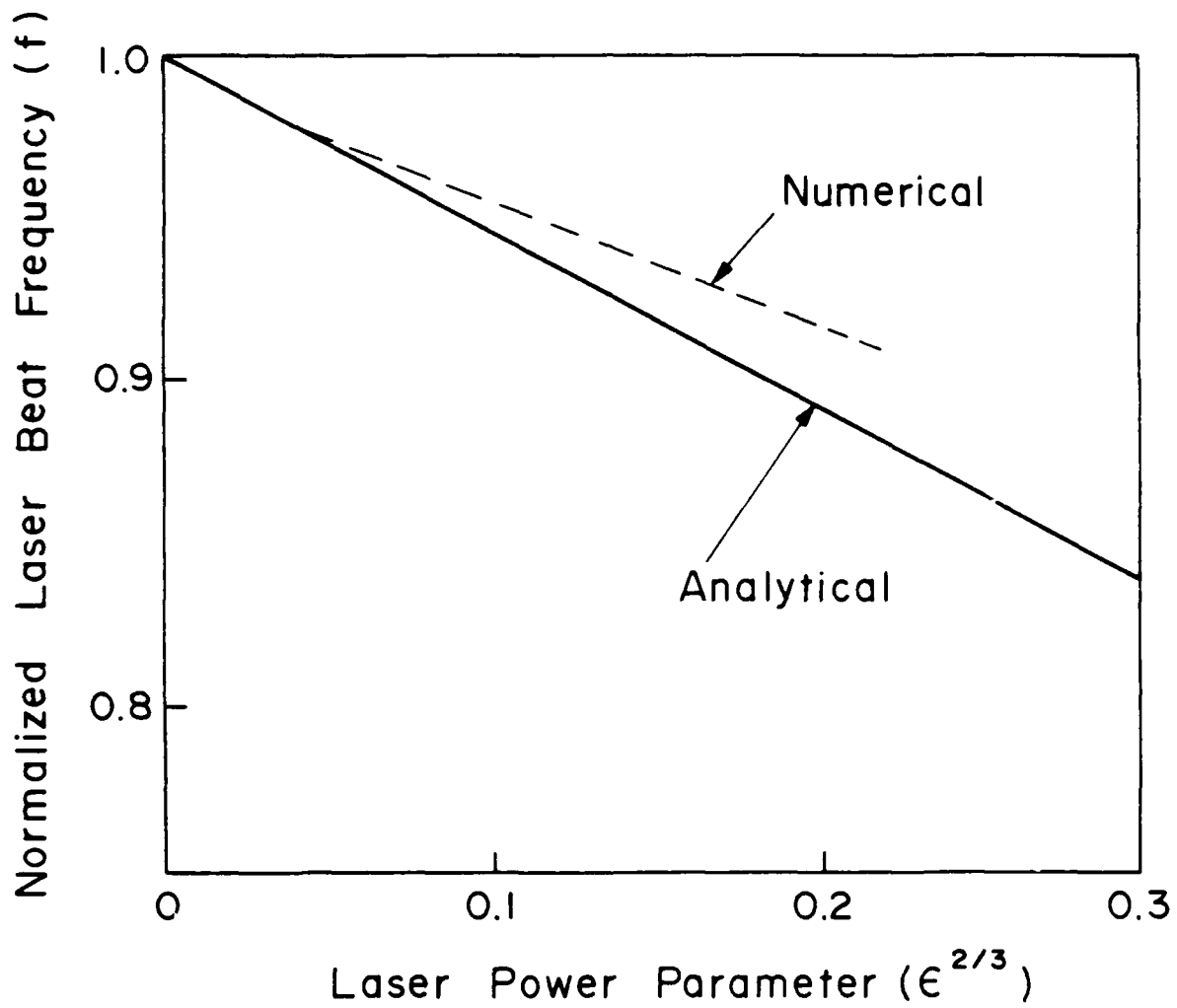
Fig. 7   Comparison of the frequency at which the largest accelerating

electric field is obtained. The solid curve is a plot of f_{opt}

obtained analytically and the dashed curve is found numerically from

the fully relativistic nonlinear equations.

37
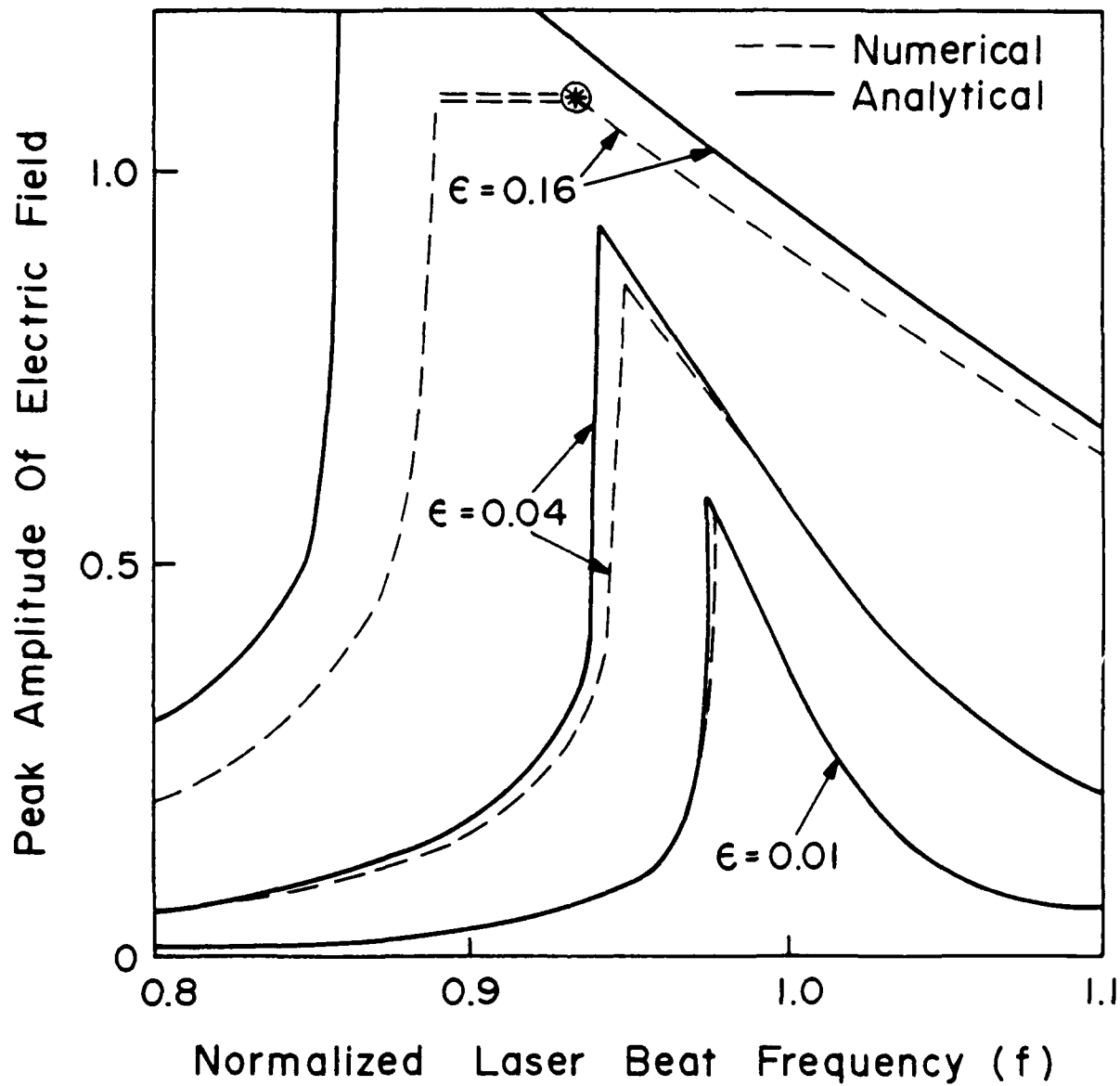
Fig. 8 Normalized peak amplitude of the accelerating electric field
for $\epsilon = 0.01$, 0.04 and 0.16 within the normalized laser beat
frequency range $0.8 < f < 1.1$. The solid curves are analytical
results of peak ΔE obtained from Eq. (34) and the dashed curves are
numerical results of peak amplitude of E obtained from the complete
analysis of Eqs. (18)–(20).
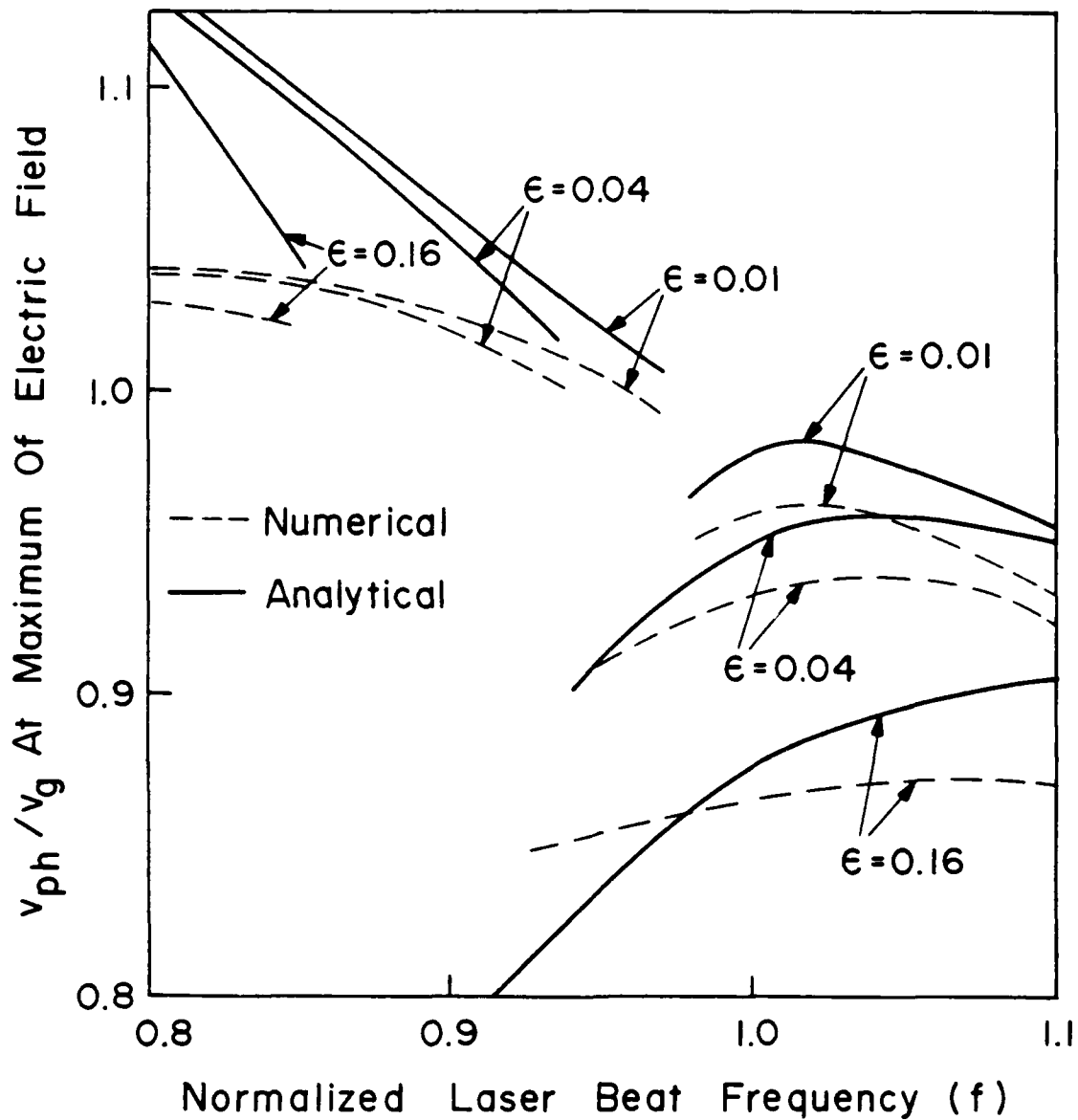
Fig. 9 Plots of the phase velocity associated with the peak electric field
for ϵ = 0.01, 0.04 and 0.16 within the normalized beat frequency
range $0.8 < f < 1.1$. The solid curves are obtained from the
analytical equations and the dashed curves are obtained from the
complete equations at the maximum of E.
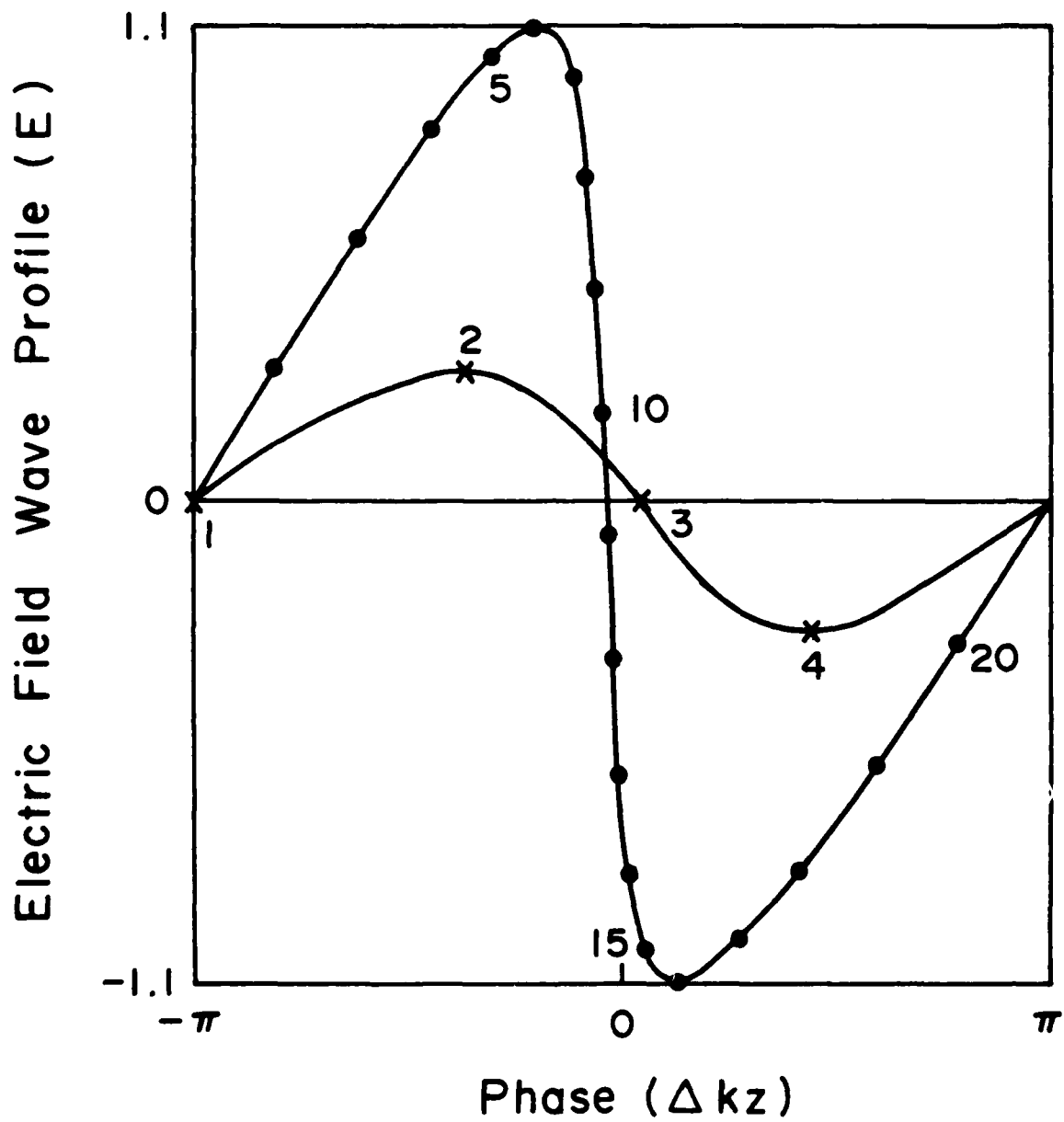
Fig. 10 Normalized electric field for one period of the laser beat wave at
two different amplitudes obtained at two different instants in time
with $\epsilon = 0.16$, $f = 0.925$ and $G = 0$, the point is marked by (*) in
Fig. 8.
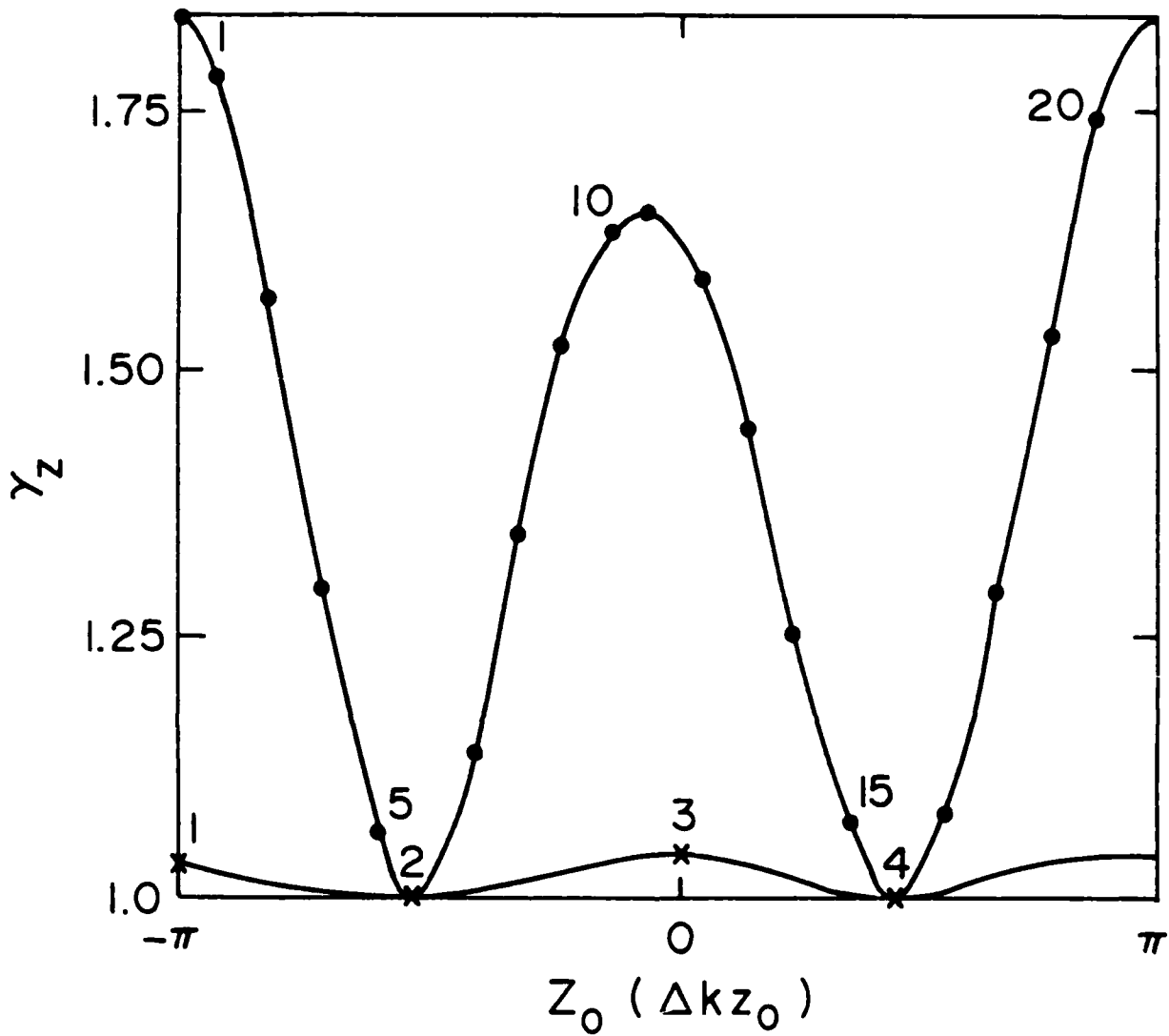
Fig. 11 Plots of the relativistic gamma associated with the axial motion γ_z for one period of the plasma oscillation for the same parameters and at the same instants in time as in Fig. 10.

41
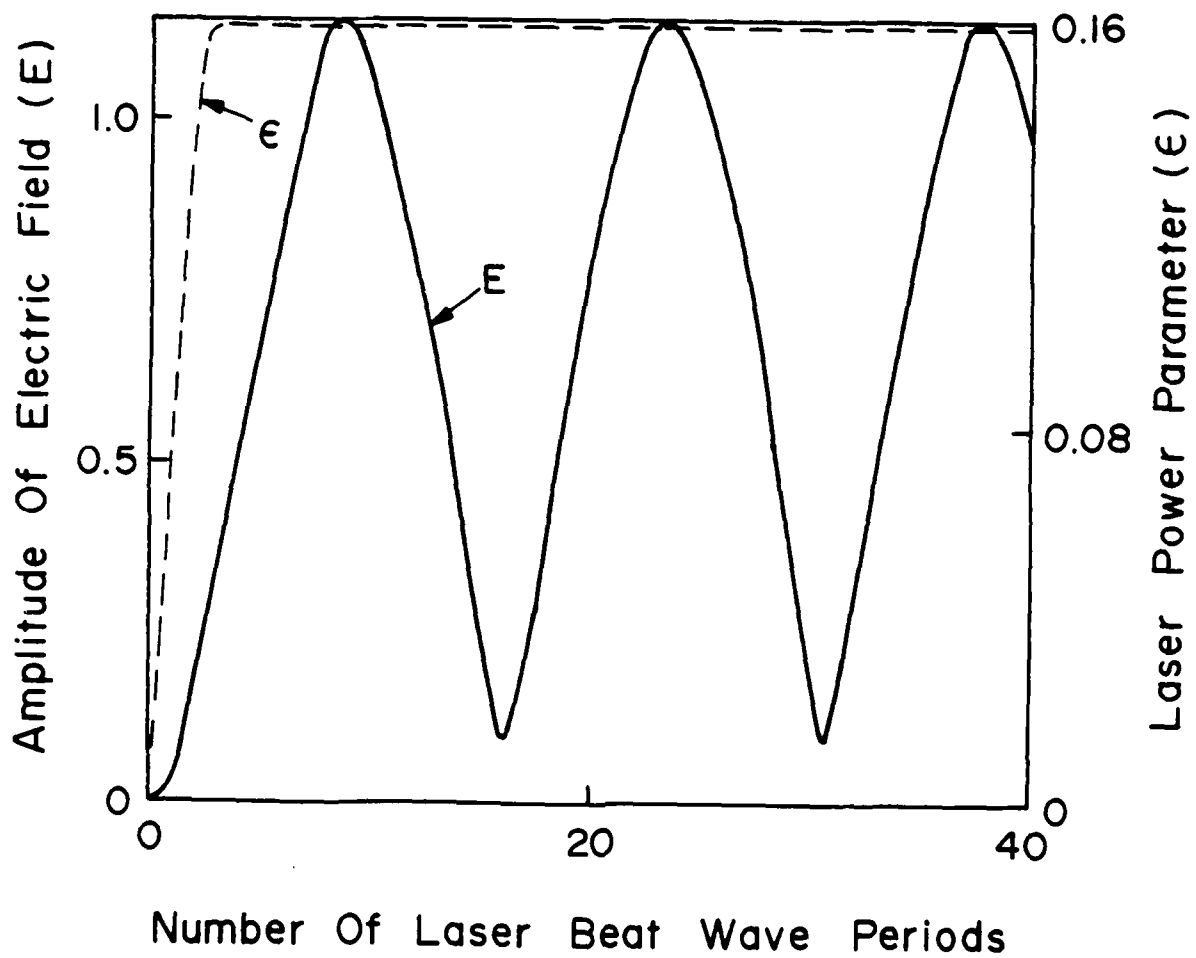
Fig. 12   Time evolution of the amplitude of the normalized electric field
(solid curve) and the time dependent laser power parameter ε (dashed
curve) for f = 0.925.
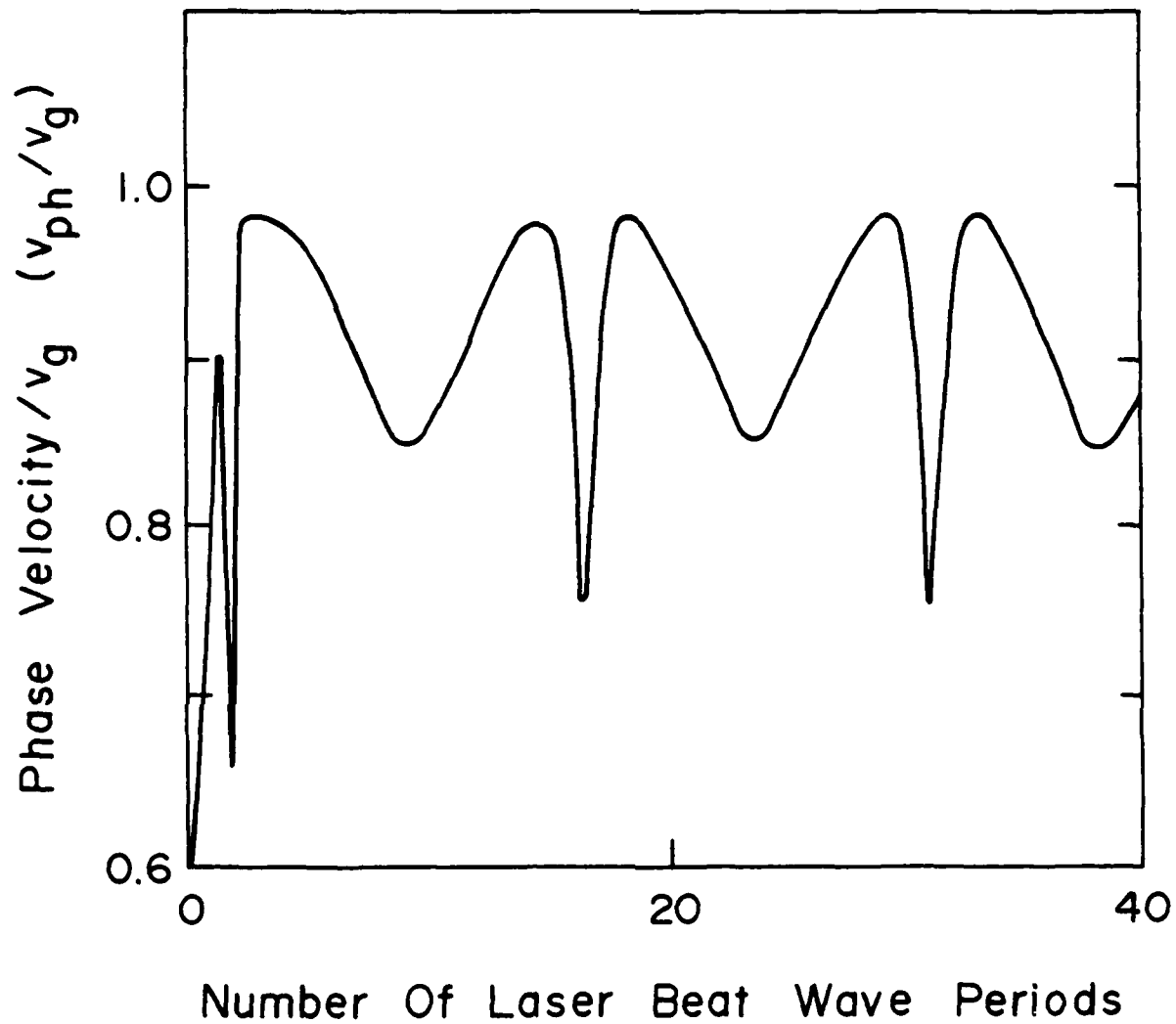
Fig. 13 The temporal dependence of the phase velocity associated with Fig. 12.
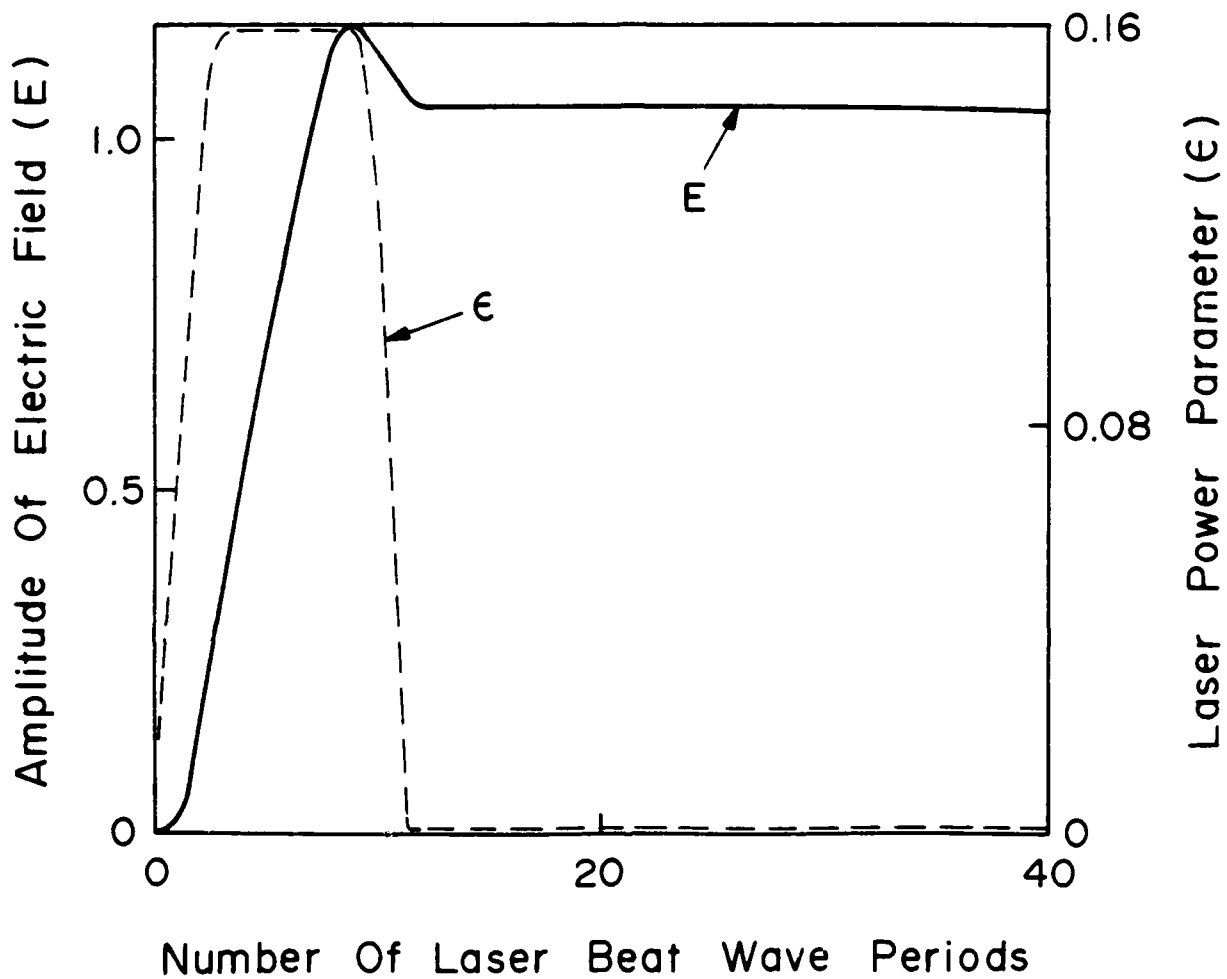
Fig. 14 The temporal evolution of the amplitude of the normalized electric field (solid curve) produced by pulsed laser beams $\epsilon(t)$ (dashed curve) for $f = 0.925$.
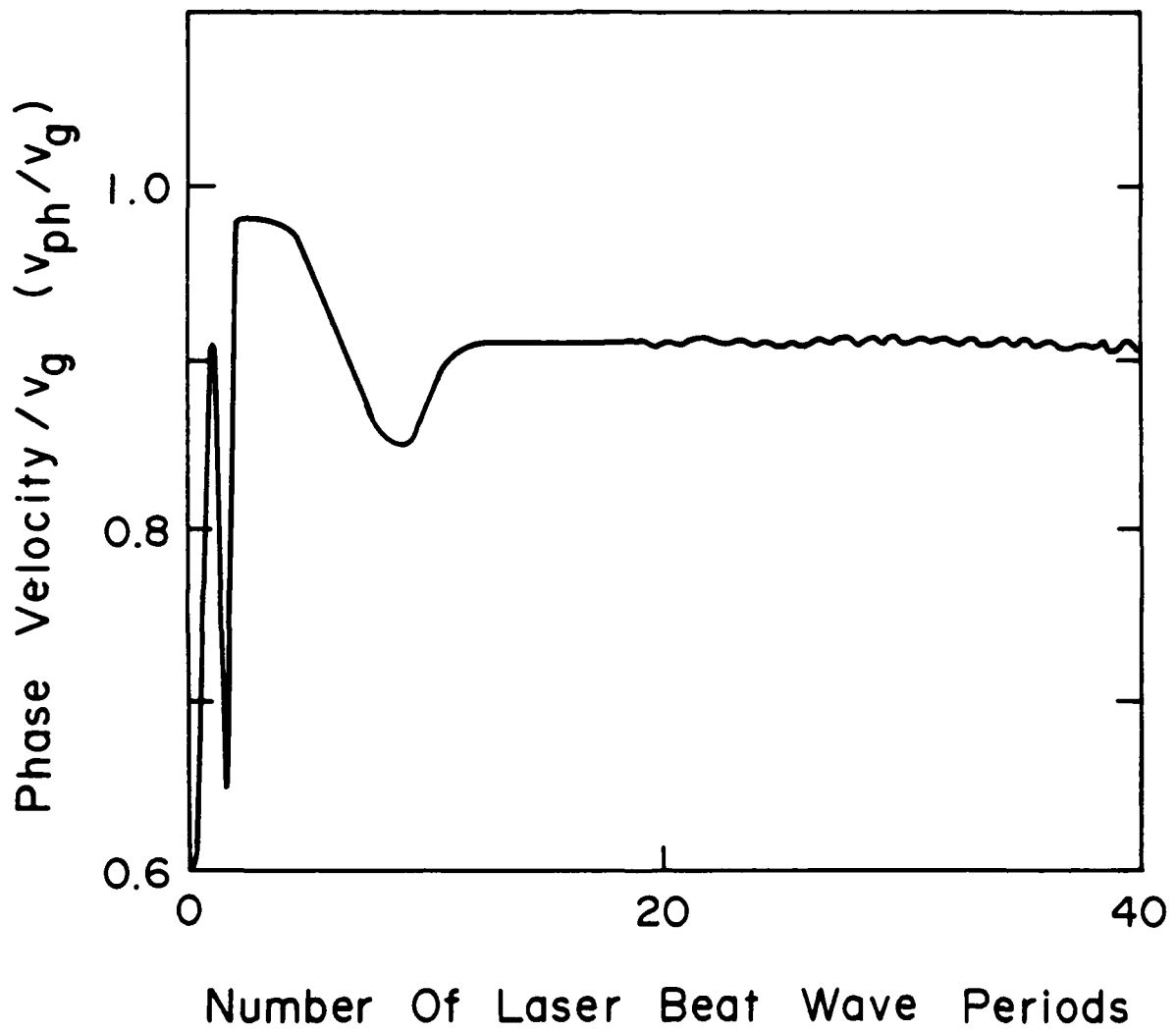
Fig. 15 The phase velocity associated with the pulsed laser beam shown in

Fig. 14.
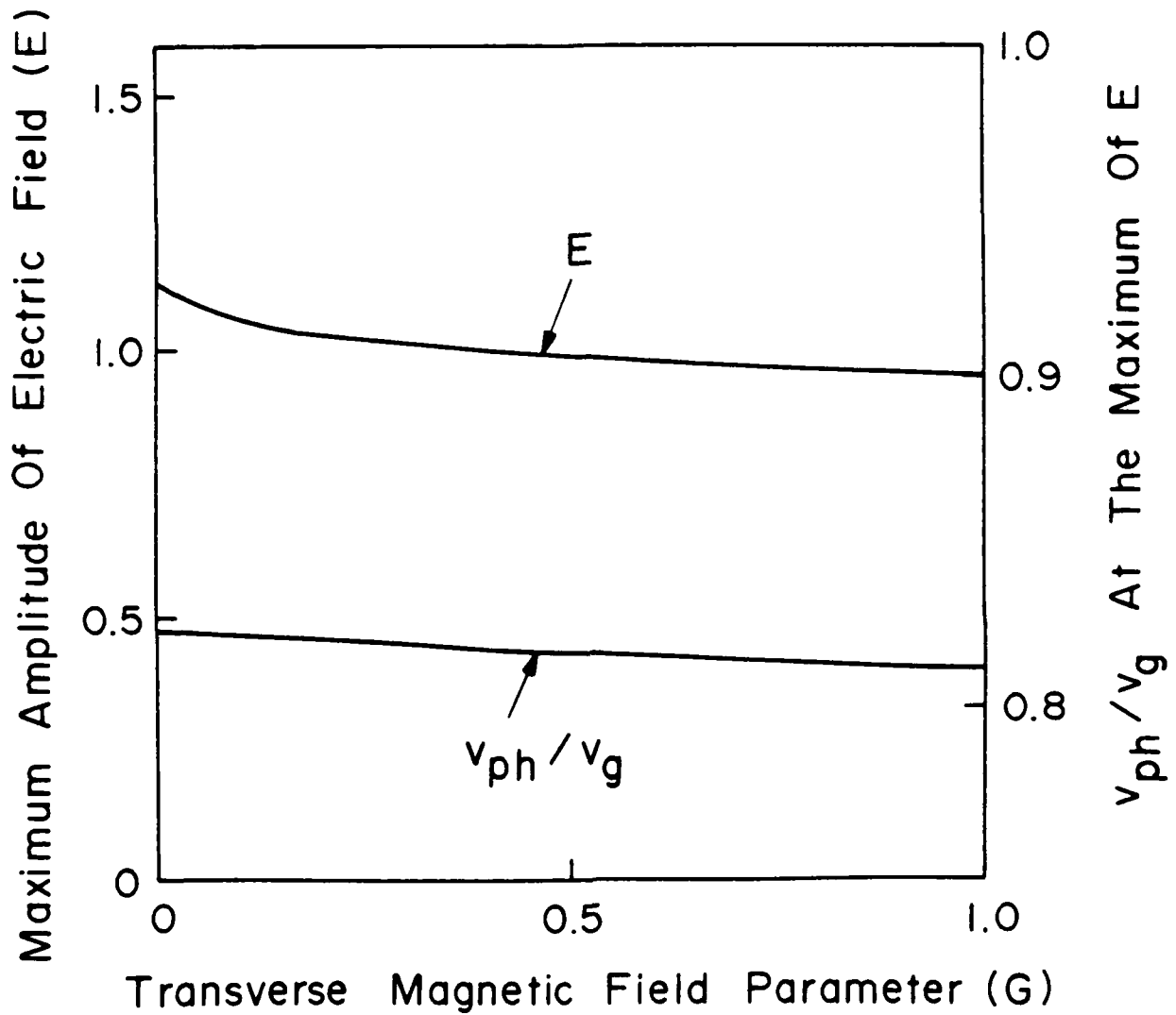
Fig. 16 Plot of the maximum amplitude of the normalized electric field E

(solid curve) and the corresponding phase velocity variation

v_{ph}/v_g (dashed curve) as a function of G for $\epsilon = 0.16$ and $f = 0.925$.
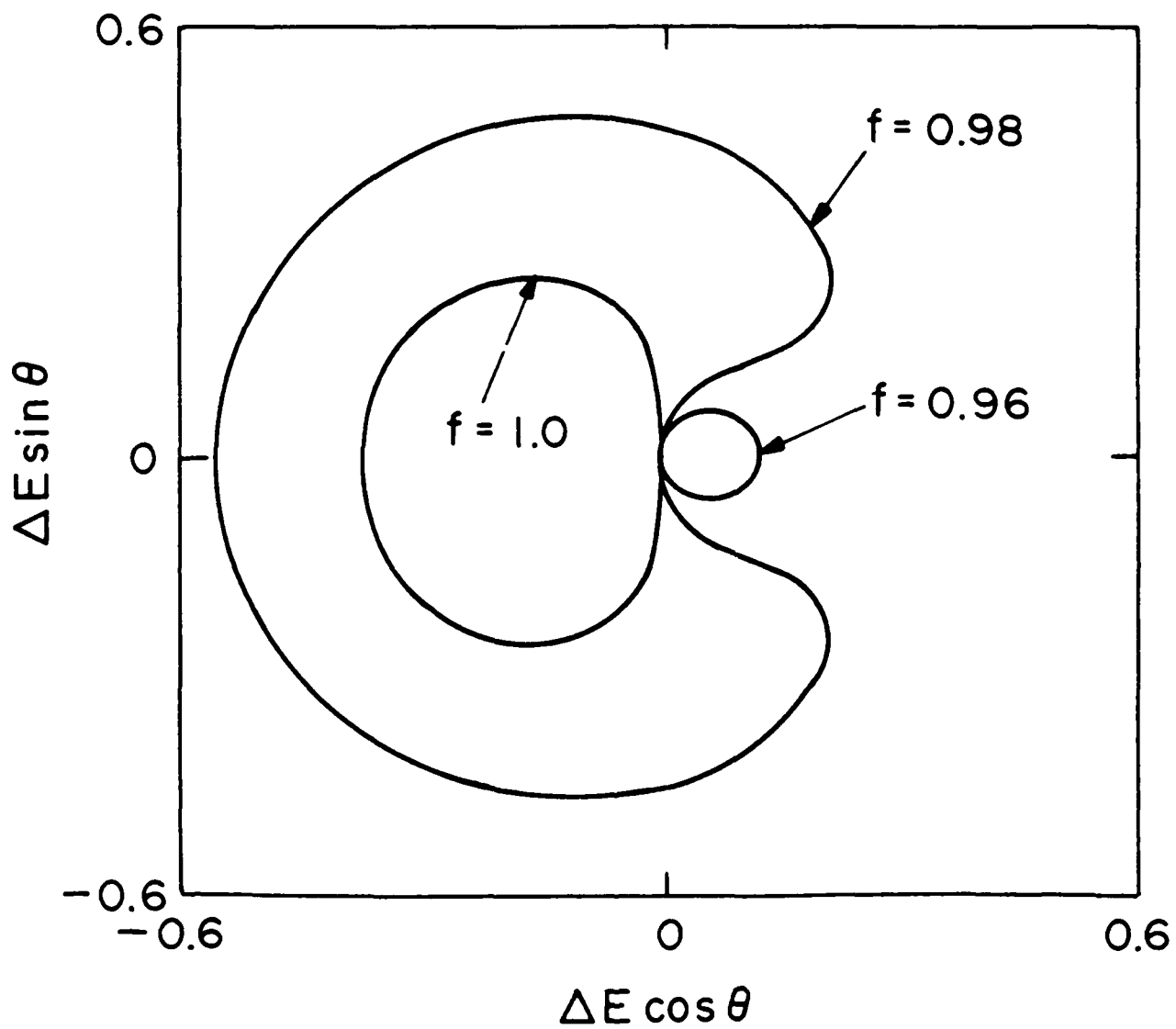
Fig. 17 Plot of $\Delta E \sin \theta$ versus $\Delta E \cos \theta$ for $\varepsilon = 0.01$, and three different normalized laser beat frequencies.

END

FILMED

2-85

DTIC